







## RESEARCH ARTICLE

# Lowering water table reduces carbon sink strength and carbon stocks in northern peatlands

Min Jung Kwon<sup>1,2</sup>  | Ashley Ballantyne<sup>1,3</sup>  | Philippe Ciais<sup>1</sup>  | Chunjing Qiu<sup>1,4</sup>  |  
 Elodie Salmon<sup>1</sup>  | Nina Raoult<sup>1</sup>  | Bertrand Guenet<sup>1,5</sup>  | Mathias Göckede<sup>6</sup>  |  
 Eugénie S. Euskirchen<sup>7</sup>  | Hannu Nykänen<sup>8</sup>  | Edward A. G. Schuur<sup>9</sup>  |  
 Merritt R. Turetsky<sup>10</sup> | Catherine M. Dieleman<sup>11</sup>  | Evan S. Kane<sup>12,13</sup> | Donatella Zona<sup>14,15</sup>

<sup>1</sup>Laboratoire des Sciences du Climat et de l'Environnement, CEA-CNRS-UVSQ, Gif-sur-Yvette, France

<sup>2</sup>Institute of Soil Science, University of Hamburg, Hamburg, Germany

<sup>3</sup>Department of Ecosystem and Conservation Science, University of Montana, Missoula, Montana, USA

<sup>4</sup>INRAE, AgroParisTech, Université Paris-Saclay, Gif-sur-Yvette, France

<sup>5</sup>Laboratoire de Géologie, Ecole Normale Supérieure, CNRS, PSL Research University, Paris, France

<sup>6</sup>Systems Department, Max Planck Institute for Biogeochemistry, Jena, Germany

<sup>7</sup>Institute of Arctic Biology, University of Alaska Fairbanks, Fairbanks, Alaska, USA

<sup>8</sup>Department of Environmental and Biological Sciences, University of Eastern Finland, Kuopio, Finland

<sup>9</sup>College of the Environment, Forestry, and Natural Sciences, Northern Arizona University, Flagstaff, Arizona, USA

<sup>10</sup>Institute of Arctic and Alpine Research, University of Colorado, Boulder, Colorado, USA

<sup>11</sup>School of Environmental Sciences, University of Guelph, Guelph, Ontario, Canada

<sup>12</sup>College of Forest Resources and Environmental Science, Michigan Technological University, Houghton, Michigan, USA

<sup>13</sup>USDA Forest Service Northern Research Station, Houghton, Michigan, USA

<sup>14</sup>Department of Animal and Plant Science, University of Sheffield, Sheffield, UK

<sup>15</sup>Department of Biology, San Diego State University, San Diego, California, USA

## Correspondence

Min Jung Kwon, Laboratoire des Sciences du Climat et de l'Environnement, CEA-CNRS-UVSQ, Gif-sur-Yvette, France.  
 Email: [minjung.kwon86@gmail.com](mailto:minjung.kwon86@gmail.com)

## Funding information

Academy of Finland, Grant/Award Number: 337550; Agence Nationale de la Recherche, Grant/Award Number: ANR-10-LABX-100-01, ANR-16-CONV-0003 and ANR-18-MPGA-0007; H2020 Societal Challenges, Grant/Award Number: 101000289 and 641816; National Science Foundation, Grant/Award Number: DEB-1026415, DEB-1636476 and LTREB-2011276

## Abstract

Peatlands at high latitudes have accumulated >400 Pg carbon (C) because saturated soil and cold temperatures suppress C decomposition. This substantial amount of C in Arctic and Boreal peatlands is potentially subject to increased decomposition if the water table (WT) decreases due to climate change, including permafrost thaw-related drying. Here, we optimize a version of the Organizing Carbon and Hydrology In Dynamic Ecosystems model (ORCHIDEE-PCH4) using site-specific observations to investigate changes in CO<sub>2</sub> and CH<sub>4</sub> fluxes as well as C stock responses to an experimentally manipulated decrease of WT at six northern peatlands. The unmanipulated control peatlands, with the WT <20 cm on average (seasonal max up to 45 cm) below the surface, currently act as C sinks in most years (58 ± 34 g C m<sup>-2</sup> year<sup>-1</sup>; including 6 ± 7 g C-CH<sub>4</sub> m<sup>-2</sup> year<sup>-1</sup> emission). We found, however, that lowering the WT by 10 cm reduced the CO<sub>2</sub> sink by 13 ± 15 g C m<sup>-2</sup> year<sup>-1</sup> and decreased CH<sub>4</sub> emission by 4 ± 4 g CH<sub>4</sub> m<sup>-2</sup> year<sup>-1</sup>, thus accumulating less C over 100 years (0.2 ± 0.2 kg C m<sup>-2</sup>).

This is an open access article under the terms of the [Creative Commons Attribution-NonCommercial](https://creativecommons.org/licenses/by-nc/4.0/) License, which permits use, distribution and reproduction in any medium, provided the original work is properly cited and is not used for commercial purposes.

© 2022 The Authors. *Global Change Biology* published by John Wiley & Sons Ltd.

Yet, the reduced emission of CH<sub>4</sub>, which has a larger greenhouse warming potential, resulted in a net decrease in greenhouse gas balance by  $310 \pm 360 \text{ g CO}_{2\text{-eq}} \text{ m}^{-2} \text{ year}^{-1}$ . Peatlands with the initial WT close to the soil surface were more vulnerable to C loss: Non-permafrost peatlands lost  $>2 \text{ kg C m}^{-2}$  over 100 years when WT is lowered by 50 cm, while permafrost peatlands temporally switched from C sinks to sources. These results highlight that reductions in C storage capacity in response to drying of northern peatlands are offset in part by reduced CH<sub>4</sub> emissions, thus slightly reducing the positive carbon climate feedbacks of peatlands under a warmer and drier future climate scenario.

#### KEYWORDS

carbon flux, carbon stock, drainage, high latitude, land surface model, manipulation experiment, permafrost thaw

## 1 | INTRODUCTION

The carbon (C) stock of northern peatlands is estimated to be 265–621 Pg (Gorham, 1991; Hugelius et al., 2020; Treat et al., 2019; Yu et al., 2010) with some estimates as high as 1055 PgC (Nichols & Peteet, 2019) despite controversy (Nichols & Peteet, 2021; Ratcliffe et al., 2021; Yu et al., 2021). Approximately half of northern peatlands are underlain by permafrost (Hugelius et al., 2020), contributing to a large portion of permafrost C stock of  $1035 \pm 150$  Pg in the first 3 m depth (Hugelius et al., 2014; Schuur et al., 2015). Most of the northern peatlands C have accumulated after the last glacial maximum (Kleinen et al., 2012; MacDonald et al., 2006; Treat et al., 2019; Yu et al., 2010), and undisturbed peatlands continue to accumulate C at present (Bridgman et al., 2006; Hugelius et al., 2020; Tarnocai et al., 2009). Peatlands act as C sinks because plant productivity sustains litter C input but anaerobic conditions, low pH, and poor litter quality inhibit peat decomposition. However, there is an increasing concern that this substantial C stock is becoming vulnerable to decomposition in response to drying. Drying, as a result of a lower water table (WT), exposes the upper peat horizons to aerobic conditions, which dramatically increases C decomposition rates.

In low to mid-latitudes, substantial areas of peatlands have become drier due to anthropogenic drainage by ditches for forestry, agriculture, and urbanization (Byrne et al., 2004; Evans et al., 2021; Wijedasa et al., 2018), in addition to climate warming and drying over natural peatlands (Swindles et al., 2019). In northern high latitudes, however, peatland drying is mostly associated with climate change through several processes. First, if evapotranspiration increases faster than precipitation, the WT is likely to decrease. Generally, increasing precipitation is expected due to an enhanced hydrologic cycle (Bintanja & Andry, 2017; Bintanja & Selten, 2014) but the patterns vary spatially and temporally (Greve et al., 2014) together with more frequent extreme precipitation events (Palmer & Räisänen, 2002; Shioyama et al., 2016). Furthermore, in the high latitudes, a large fraction of precipitation can be lost during

the spring melt (Douville et al., 2021; Kirtman et al., 2013) and the growing season can have a negative water balance. Coupled Model Intercomparison Project (CMIP6) climate models predict shorter but stronger drought events at high latitudes by 2100 (Ukkola et al., 2020). Warmer temperatures also enhance evapotranspiration (Helbig et al., 2020), which decreases soil moisture, and possibly the WT in peatlands. Second, higher air temperatures thaw permafrost and melt extensive ground ice complexes, which subsequently increases active layer thickness and changes surface morphology. This change in surface morphology alters the spatial and vertical distribution of water in permafrost peatlands and exposes surface peat layers to aerobic decomposition in some areas (Lewis et al., 2012; Olefeldt et al., 2016). This can occur at small spatial scales, with a variation of local wet versus dry patches in polygonal tundra, or at large scales, such as thermokarst formation or thaw lake drainage, which are highly variable in space and time (Fewster et al., 2022; Jones et al., 2022; Liljedahl et al., 2016).

Currently, Arctic and boreal peatlands are C sinks (Virkkala et al., 2021), and peatland drying has the potential to alter C fluxes and soil organic C (SOC) stocks (Avis et al., 2011; Lara et al., 2015; Lawrence et al., 2015; Vaughn et al., 2016; Wainwright et al., 2015). Generally, the exposure of peat soils to oxygen in the undersaturated part of the soil profile decreases CH<sub>4</sub> production and emissions but increases CO<sub>2</sub> emissions due to SOC decomposition (Huang et al., 2021; Leifeld et al., 2019; Leifeld & Menichetti, 2018), potentially contributing to a positive carbon-climate feedback (Günther et al., 2020). Huang et al. (2021) estimated CO<sub>2</sub> emissions to be increased by  $1.12 \text{ mg C m}^{-2} \text{ h}^{-1} \text{ cm}^{-1}$  and CH<sub>4</sub> emissions to be decreased by  $0.09 \text{ mg C m}^{-2} \text{ h}^{-1} \text{ cm}^{-1}$  due to drying in global peatlands, but the emission changes of northern peatlands were highly sensitive and variable compared to lower latitudes. In addition, temperature sensitivity of CH<sub>4</sub> emissions varies with WT and can add complexity to the CH<sub>4</sub>:CO<sub>2</sub> ratio under temperature and WT variations (Chen et al., 2021).

Despite growing research on the sensitivity of peatlands to drying, both CO<sub>2</sub> and CH<sub>4</sub> gas responses and the change of C

stocks in northern circumarctic peatlands are still uncertain, especially for peatlands underlain by permafrost. Individual-site studies in Arctic and Boreal regions consistently showed increased CO<sub>2</sub> emissions from ecosystem respiration ( $R_{\text{eco}}$ , [Kittler et al., 2016; Martikainen et al., 1995; Natali et al., 2015]) and decreased CH<sub>4</sub> emissions (Kittler et al., 2017; Kwon et al., 2017; Natali et al., 2015; Nykänen et al., 1998; Olefeldt et al., 2017; Turetsky et al., 2008, 2014; Zona et al., 2009) in response to lower WT. However, gross primary production (GPP) showed contrasting responses, that is, reduced (Olefeldt et al., 2017) or increased GPP (Kittler et al., 2016; Natali et al., 2015), depending on the plant community composition and the occurrence of shift in species due to drying. Some studies synthesized the drying effects in northern circumarctic peatlands, but they were limited to CH<sub>4</sub> (Nykänen et al., 1998; Olefeldt et al., 2013; Turetsky et al., 2014) or to a small region (Laine et al., 1996). To quantify the response of both CO<sub>2</sub> and CH<sub>4</sub> fluxes and SOC stock to drying in northern peatlands, we compiled CO<sub>2</sub> and CH<sub>4</sub> fluxes from six field WT manipulation experiments from Arctic and Boreal sites, optimized key parameters of the ORCHIDEE-PCH4 land surface model using data assimilation to reproduce varying WT conditions, and quantified the C flux and stock change in response to drying. Specifically, using a site specifically optimized model, we first quantify the sensitivity of C fluxes of each site when WT is sequentially lowered by 5, 10, 20, and 50 cm relative to the control WT, and then evaluate the changes in C stocks when the WT is lowered for 100 years. Lastly, we compare what drives the variations in C flux sensitivity among sites.

## 2 | METHOD

### 2.1 | Field drying manipulation experiment sites

We used data from six field WT manipulation (drainage) experiments, which are located between 62- and 71-degree North: (1) Särkkä, Finland (FI-SAR), (2) Lakkasuo, Finland (FI-LAK), (3) Healy, Alaska (US-HEA), (4) Bonanza, Alaska (US-BZF), (5) Chersky, Russia (RU-CHE), and (6) Utqiagvik (a.k.a. Barrow), Alaska (US-BES; Table 1). The specific peatland types include boreal bog, fen, and moist/wet tundra. Three sites are underlain by permafrost, while the others are not (Table 1). Peat depths range from 0.2 to 2.7 m (Table 2; note that RU-CHE has peat depths of 0.2–0.4 m considering spatial heterogeneity, and to be exact it is not peatland by definition—peat depth should be >0.4 m). The average control WT varies from 20 cm (belowground) to –5 cm (aboveground), with the lowest seasonal WT ranging from 45 cm to –1 cm (Figure S1). The drainage experiments were carried out in parallel with the control experiments, and the drainage intensity varies by site, ranging from –17 (17 cm lower WT compared to the control) to 0 cm (no average difference). Flux rates were measured 0–30 years after the drying experiments started. CO<sub>2</sub> and CH<sub>4</sub> fluxes were measured using eddy covariance method and/or chambers. More details on

TABLE 1 Site characteristics of northern peatlands with field drying manipulation experiments used for the model calibration

Site (abb)	Latitude	Longitude	Ecosystem type	Permafrost presence	MAT (°C)	MAP (mm)	Drained since	Flux measurement (observation years)	Gas measured	Ref.
Särkkä, Finland (FI-SAR)	61.79	24.28	Bog	No	1.9	650	1978	Ch (1991–92)	CO <sub>2</sub> , CH <sub>4</sub>	Nykänen et al. (1998)
Lakkasuo, Finland (FI-LAK)	62.80	30.98	Fen + bog	No	3.0	709	1961	Ch (1991–92)	CO <sub>2</sub> , CH <sub>4</sub>	Nykänen et al. (1998)
Healy, Alaska (US-HEA)	63.88	–149.23	Moist tundra	Yes	–1.0	378	2011	Ch (2011–18) Ch (2016–18)	CO <sub>2</sub> CH <sub>4</sub>	Natali et al. (2015)
Bonanza, Alaska (US-BZF)	64.70	–148.33	Fen	No	–2.2	100	2005	EC (2011–18) Ch (2005–18) EC (2014–18) Ch (2005–18)	CO <sub>2</sub> CO <sub>2</sub> CH <sub>4</sub> CH <sub>4</sub>	Euskirchen et al. (2020); Olefeldt et al. (2017)
Chersky, Russia (RU-CHE)	68.62	161.35	Wet tundra	Yes	–11.0	197	2004	EC (2014–16)	CO <sub>2</sub> , CH <sub>4</sub>	Göckede et al. (2019); Kittler et al. (2017)
Utqiagvik, Alaska (US-BES)	71.28	–156.60	Wet tundra	Yes	–12.0	173	2007	EC (2006–07)	CO <sub>2</sub> , CH <sub>4</sub>	Zona et al. (2009, 2012)

Abbreviations: Ch, chamber; EC, eddy covariance; MAP, mean annual precipitation; MAT, mean annual temperature.

TABLE 2 Initialization parameters for each site for fitting soil temperature and soil organic carbon (C) content

Site	# dry peat layer (cm)	SOC accumulation (years)	obs. peat depth (m)	sim. peat depth (m)	obs.SOC (kg C m <sup>-2</sup> )	sim.SOC (kg C m <sup>-2</sup> )
FI-SAR	3 (1.0)	800	2.7	2.0	71–78	77
FI-LAK	2 (0.4)	700	2.3	2.0	71–78	76
US-HEA	4 (2.1)	800	0.35–0.45	1.5	19–31	35
US-BZF	2 (0.4)	800	1–2	1.5	-	53
RU-CHE	3 (1.0)	8000	0.2–0.4	0.7	12–24	24
US-BES	0 (0.0)	2000	1	1.5	16–31	34

Note: The number of dry peat layers (and corresponding thickness in cm) was included to increase goodness of fit between simulated and observed soil temperature, which does not influence the actual WT or soil moisture. Simulated peat depth and SOC are from the corresponding observation years for comparison to the observations, and may differ over the simulation years. The amount of SOC was simulated by adjusting the number of spin-up years, that is, SOC accumulation years.

site characteristics and experimental setups are found in the references in Table 1.

## 2.2 | Model description

We used a modified version of the land surface model ORCHIDEE-PEAT that was developed to simulate northern peatlands (Qiu et al., 2018). This version is called ORCHIDEE-PCH4, and simulates hydrology, surface energy, and C cycle processes resulting in CO<sub>2</sub> and CH<sub>4</sub> fluxes in northern peatlands using the parameterizations from Qiu et al. (2018) and a CH<sub>4</sub> module (Salmon et al., 2021). Photosynthesis and plant respiration are simulated for peatland vegetation type (represented as C3 graminoids) as described in section 2.2.1 in Qiu et al. (2018). After senescence, litterfall goes into two litter pools (metabolic and structural) and three soil C pools (active, slow, and passive) after a series of decomposition processes following the CENTURY scheme (Krinner et al., 2005; Parton et al., 1987; Paustian et al., 1992). The decomposition rates of active, slow, and passive soil C pools, including the transfer among soil pools are 1.0, 0.027, and 0.0006 year<sup>-1</sup> at 30°C, and the actual rates are simulated considering soil temperature, moisture, and depth (Qiu et al., 2019). Peat C from three pools is decomposed to CO<sub>2</sub> and CH<sub>4</sub>, with the decomposition rates affected by soil temperature and moisture, peat depth, and additionally oxygen concentration in soil pores in the case of CH<sub>4</sub> (Qiu et al., 2019; Salmon et al., 2021). Oxygen is diffused between the atmosphere and the top soil layer, or through snow layers when existing, as well as between soil layers, and is also provided up to the rooting depths by plant roots (Salmon et al., 2021). Oxygen in soils oxidizes CH<sub>4</sub>, and the oxidation rate is determined by the turnover time of CH<sub>4</sub> (Salmon et al., 2021). The residual CH<sub>4</sub> after oxidation in each layer is then emitted to the atmosphere through diffusion, ebullition, and plant-mediated transport. Diffusion occurs between soil layers as well as between top soil layer and the atmosphere based on the concentration gradients, soil moisture, and soil pore size. Methane bubbles form due to hydrostatic pressure in soil, and the probability of these bubbles to reach the atmosphere is simulated as ebullition. The amount of plant-mediated transport is

influenced by the gas transport efficiency (representing aerenchyma density) and seasonal plant productivity. More details on these processes are described in section 2.1 in Salmon et al. (2021). Peat growth (accumulation of peat C; C input into soil minus CO<sub>2</sub> & CH<sub>4</sub> production/decomposition) is simulated by transferring excessive peat C of one layer to the one below within the 32 discretized soil layers (section 2.1 in Qiu et al. (2019)).

## 2.3 | Model setup and parameter optimization

The ORCHIDEE model allows multiple vegetation types in one grid cell, with distinct soil tiles to compute the hydrology of peat, herbaceous, and woody vegetation types. The fraction of the grid cell occupied by peatland receives runoff from the other non-peat vegetation fractions to maintain a high WT (Qiu et al., 2018), and the prognostic WT in peatland depends on the fraction size of non-peatland vegetation. Here, we do not use the prognostic WT from the model but set the entire grid cell to be covered by peatlands. Then, we prescribed soil moisture according to the observed daily WT (the resolution can be 30 min), and set soil moisture to 0.80 (80% of soil porosity filled with water and 20% with air) for the soil layers below WT and to 0.50 for the soil layers above WT. These values are the averages soil moisture observed in US-HEA and RU-CHE sites, where volumetric soil moisture was measured.

To more accurately simulate soil temperature, which is one of the critical drivers for CO<sub>2</sub>- and CH<sub>4</sub>-related processes and their rates, we used the thermal properties (heat capacity of 2.5·10<sup>6</sup> JK<sup>-1</sup> m<sup>-3</sup> and thermal conductivity of 0.05 W m<sup>-1</sup> K<sup>-1</sup> [dry] and 0.25 W m<sup>-1</sup> K<sup>-1</sup> [solid]) of 100% organic soil in the model. The apparent heat capacity and thermal conductivity were calculated considering the water and ice content in soil (Guimberteau et al., 2018). Plus, when simulated soil temperature was higher than observations, we overwrote the thermal properties of dry peat soils at the top soil layers within the soil thermic sub-module to mimic the insulating function of an overlying moss or organic soil layer to accurately simulate observed soil temperature profiles (Gornall et al., 2007; Soudzilovskaia et al., 2013)

as in (Ekici et al., 2014). These dry peat layers were decoupled from the soil hydrology module and only used for simulating soil temperature profiles. The number of dry peat layers was optimized for each site by minimizing the root mean squared error (RMSE) and Nash-Sutcliffe model efficiency coefficient (MEF) from the observed soil temperatures (shown in Table 2 and Figure S2).

We calibrated the key parameters that are associated with CO<sub>2</sub> and CH<sub>4</sub> fluxes to simulate site-specific fluxes of the control treatment (Table 3). Thus, the differences in C fluxes between control and dry treatments are driven by the prescribed WT of each treatment and model parameters that change by soil moisture. For GPP, the V<sub>c<sub>max</sub></sub> at 25°C (maximum carboxylation rate in photosynthesis at 25°C; default 40 μmol m<sup>-2</sup> s<sup>-1</sup> [Qiu et al., 2018]) was calibrated. In default setting, GPP decreases with decreasing soil moisture availability. However, some plants can photosynthesize more actively under dry condition (Sulman et al., 2010). In addition, some sites (e.g., RU-CHE) showed significant changes in vegetation communities due to drying, with greater shrub abundance (Kwon et al., 2016) and GPP (Kittler et al., 2016). Increasing shrub abundance is often observed in drying northern peatlands unless taller trees outcompete them for light (Harris et al., 2020; Laiho et al., 2003; Murphy et al., 2009). To test the effects of increased photosynthetic rates on flux and stock change with or without composition changes, we additionally ran simulations with the increased V<sub>c<sub>max</sub></sub> at 25°C by 10% to mimic increased plant productivity. The phenology was selected between C<sub>3</sub> grasses and C<sub>3</sub> grasses + mosses by minimizing errors (RMSE and MEF) between simulations and observations. Phenology determines the onset time of photosynthesis, with the earlier onset when mosses are present, as they can photosynthesize at lower temperature and lower light level than C<sub>3</sub> grasses (Atanasiu, 1971). The growing degree days (GDD) threshold for the onset of C<sub>3</sub> grass photosynthesis is calculated using

$$\text{GDD threshold} = 320 + 6.25 \cdot \text{temp} + 3.125 \cdot 10^{-2} \cdot \text{temp}^2 \quad (1)$$

where temp is the average air temperature of the past 3 years. The coefficients of Equation (1) are calibrated globally for different vegetation types (Botta et al., 2000; Krinner et al., 2005). Earlier onset of

photosynthesis for C<sub>3</sub> grasses + mosses is achieved by reducing the threshold of GDD using

$$\text{GDD threshold} = \frac{1.93 \cdot 10^5}{\left(1 + e^{\left(-8.13 \cdot 10^{-2} \cdot (\text{temp} - 87.87)\right)}\right)} \quad (2)$$

which is calibrated by GPP observations in 19 northern peatlands (Qiu et al., 2018). Different from the default setting of respiration (CO<sub>2</sub> production) cutoff below -1°C, we allowed a continuous CO<sub>2</sub> respiration at sub-zero temperatures, with the temperature control on respiration using.

$$\text{Temperature control} = e^{\left(\frac{0.69 \cdot (\text{soil temperature} - 30)}{10}\right)}, \text{max} = 1 \quad (3)$$

as non-growing season respiration can be considerable (Natali et al., 2019).

The amount of plant-mediated CH<sub>4</sub> transport was calculated after subtracting the fixed fraction of methanotrophy at roots (mrox in the equation 9 in Salmon et al. (2021)) in the original model. Instead, we excluded the methanotrophy (mrox) term in the plant-mediated CH<sub>4</sub> transport equation but used mrox as the amount of oxygen provided into soil through roots, and let it oxidize CH<sub>4</sub> during the methanotrophy process in soils, similar to Morel et al. (2019). This allowed the amount of plant-mediated CH<sub>4</sub> transport decoupled from methanotrophy in soils. Then, six parameters were optimized targeting the best fit to the observed CH<sub>4</sub> emissions of control treatment of each site using the ORCHIDEE Data Assimilation Systems (ORCHIDAS; Bastrikov et al. (2018); <https://orchidas.lsce.ipsl.fr/>). Daily CH<sub>4</sub> emissions of growing season were linearly interpolated for days without observations, and the earliest (latest) observations of each year were used for CH<sub>4</sub> emissions before (after) the first (last) observation of that year. Within the ORCHIDAS framework, we used the genetic algorithm (Goldberg & Holland, 1988; Haupt & Haupt, 2004) to find the best set of parameters within the defined boundary of each parameter. This stochastic algorithm is a global random search method based on the principles of genetics and natural selection, and was found in Bastrikov et al. (2018) to outperform traditional

**TABLE 3** Parameter sets for each site for fitting CO<sub>2</sub> and CH<sub>4</sub> fluxes: V<sub>c<sub>max</sub></sub> at 25°C (maximum carboxylation rate in photosynthesis at 25°C), k (methanogenesis rate relative to the oxic decomposition), k<sub>MT</sub> (turnover time of methanotrophy), tveg (the amount of CH<sub>4</sub> transported through aerenchymatous plants), mrox (the amount of oxygen provided into soil through roots), mxr (the mixing ratio of CH<sub>4</sub> in bubbles in soils), and wsize (the extent of the connected network of water-filled pores)

Site	V <sub>c<sub>max</sub></sub> (μmol m <sup>-2</sup> s <sup>-1</sup> )	Phenology	k (ratio to oxic decomposition)	k <sub>MT</sub> (s)	tveg	mrox	mxr (fraction)	wsize (m)
FI-SAR	40	C <sub>3</sub> + moss	4.92	129,047	0.10	1.30	0.05	0.49
FI-LAK	40	C <sub>3</sub> + moss	4.56	86,400	0.25	1.03	0.07	0.48
US-HEA	40	C <sub>3</sub>	9.82	153,127	0.41	0.39	0.52	0.24
US-BZF	45	C <sub>3</sub>	6.65	86,400	1.30	0.5	0.20	0.38
RU-CHE	40	C <sub>3</sub>	1.02	97,695	2.23	1.07	0.11	0.41
US-BES	40	C <sub>3</sub> + moss	2.00	161,472	3.71	0.70	0.39	0.05

Note: The parameters related to CH<sub>4</sub> processes are optimized using the ORCHIDAS.

gradient-based approaches when optimizing key ORCHIDEE model parameters. Calibrated parameters include  $k$  (methanogenesis rate relative to the oxic decomposition; for example,  $k$  of 2 represents the  $\text{CO}_2$  and  $\text{CH}_4$  maximum production ratio of 2:1; ranging from 1 to 10; Khvorostyanov et al., 2008; Wania et al., 2010),  $k_{\text{MT}}$  (turnover time of methanotrophy; ranging from 1 to 5 days; Juncher Jørgensen et al., 2014; Khvorostyanov et al., 2008; Morel et al., 2019),  $t_{\text{veg}}$  (the amount of  $\text{CH}_4$  transported through aerenchymatous plants; ranging from 0 to 30; Walter & Heimann, 2000),  $m_{\text{rox}}$  (the amount of oxygen provided into soil through roots, which can oxidize  $\text{CH}_4$  in soils; ranging from 0 to 5, Walter & Heimann, 2000),  $m_{\text{xr}}$  (the mixing ratio of  $\text{CH}_4$  in bubbles in soils; ranging from 0.05 to 0.53; Baird et al., 2004; Morel et al., 2019; Riley et al., 2011), and  $w_{\text{size}}$  (the extent of the connected network of water-filled pores that affects the probability of  $\text{CH}_4$  bubbles to reach the soil surface; ranging from 0.001 to 0.5; Khvorostyanov et al., 2008) are summarized in Table 3. The range of each parameter was defined and modified following Salmon et al. (2021), which evaluated  $\text{CH}_4$  fluxes across 14 northern peatlands. Optimized parameter sets were used during the experimental simulations (at the start of the drying experiment; described in the next section). The first 20 years of simulations were excluded, which may include transitional status due to changed parameters.

## 2.4 | Model simulations of each site

The simulation was forced by the measured meteorology of random years at each site on a 30-min time-step. When meteorological measurements were not available, they were substituted by CRUNCEP v8 for the corresponding grid cell for the site-specific observation years ([https://vesg.ipsl.upmc.fr/thredds/catalog/work/p529viov/cruncep/V8\\_1901\\_2016/catalog.html](https://vesg.ipsl.upmc.fr/thredds/catalog/work/p529viov/cruncep/V8_1901_2016/catalog.html)). The model simulations were performed as follows: (1) the full model was run for 50 years to obtain steady state daily values for soil C inputs, (2) a soil accumulating spin-up sub-model was run for a site-specific time period to match simulated SOC content with observed SOC (Table 2), and (3) another 50 years of the full model run was conducted to achieve the equilibrium of physical variables. During the spin-up, atmospheric ( $\text{CO}_2$ ) was set to the pre-industrial level of 286 ppm, and (4) transient simulations were carried out with the observed rising atmospheric [ $\text{CO}_2$ ] for 100 years until the starting year of drying experiment. During the simulations, WT was prescribed with the site-specific daily WT of the control treatment.

Afterwards, another 100 years of experimental simulations were conducted at each site, using (a) the WT of the control sites (Figure S1), (b) the WT of the dried sites (Figure S1), and (c) the WT sequentially lowered by 5, 10, 20, and 50 cm relative to the WT of the control sites. Sequential drying was applied until the WT did not exceed the maximum thaw depth for permafrost-affected peatlands, which was equivalent to a WT depth 20 cm lower than controls, and until the WT up to 50 cm belowground for non-permafrost peatlands because hydrological self-regulation of peatlands may not sustain low WT in the long term (Dise, 2009; Waddington et al., 2015).

When WT and fluxes were measured at multiple locations within the study site (chamber-based method), we used the average WT for one representative simulation of that site. In addition, we excluded sub-plots, which experienced significant tree growth following drying (two sub-plots were excluded out of six in the case of FI-LAK).

## 2.5 | Model-observation comparison and statistical analysis

Model simulation errors against observations were estimated: RMSE, and the squared of its two partitioned components, squared difference of standard deviations (SDSD) and the lack of positive correlation weighted by the standard deviation (LCS) following Kobayashi and Salam (2000). They measure the magnitudes, for example, maximum and minimum seasonal flux rates, and patterns of fluctuations, for example, seasonality, respectively. We also estimated MEF for each site and treatment. When the model simulation is fully matching with the observation, RMSE, SDSD, and LCS are 0 and MEF is 1.

To compare the flux sensitivity to drying, we fitted exponential equations for NEE (net ecosystem  $\text{CO}_2$  exchange;  $R_{\text{eco}} - \text{GPP}$ ) and  $\text{CH}_4$  for each site with the sequential drying.

$$\text{NEE or } \text{CH}_4 = a * e^{(b * \text{WT})} \quad (4)$$

using the nls fit function in R (R Development Core Team, 2013).

## 2.6 | Combined effects of $\text{CO}_2$ and $\text{CH}_4$

Using the new global warming potential metrics (GWP\*; Allen et al., 2018; Cain et al., 2019; Lynch et al., 2020), we estimated the combined effects of  $\text{CO}_2$  and  $\text{CH}_4$  flux changes. Different from the conventional GWP, GWP\* considers the removal of short-lived gases over time, for example, the removal of  $\text{CH}_4$  from the atmosphere after the residence time of 12 years. Thus, its application can be especially beneficial when the  $\text{CH}_4$  emission is stable or decreasing over time.

# 3 | RESULTS

## 3.1 | Comparison between observations and simulations

The model simulated soil temperature profiles well (Figure S2). Although peat pore  $\text{CO}_2$  and  $\text{CH}_4$  concentrations can vary with WT and site-specific characteristics, simulated concentrations (ca. 3–40 g  $\text{CH}_4 \text{ m}^{-2}$ ) were comparable with those of the previous studies (Saarnio et al., 1997; Waddington et al., 2009). Together with the prescribed WT, reasonable soil temperature and pore gas concentrations, and calibration of flux-related parameters, model simulations and observations of daily  $\text{CO}_2$  and  $\text{CH}_4$  fluxes agreed well



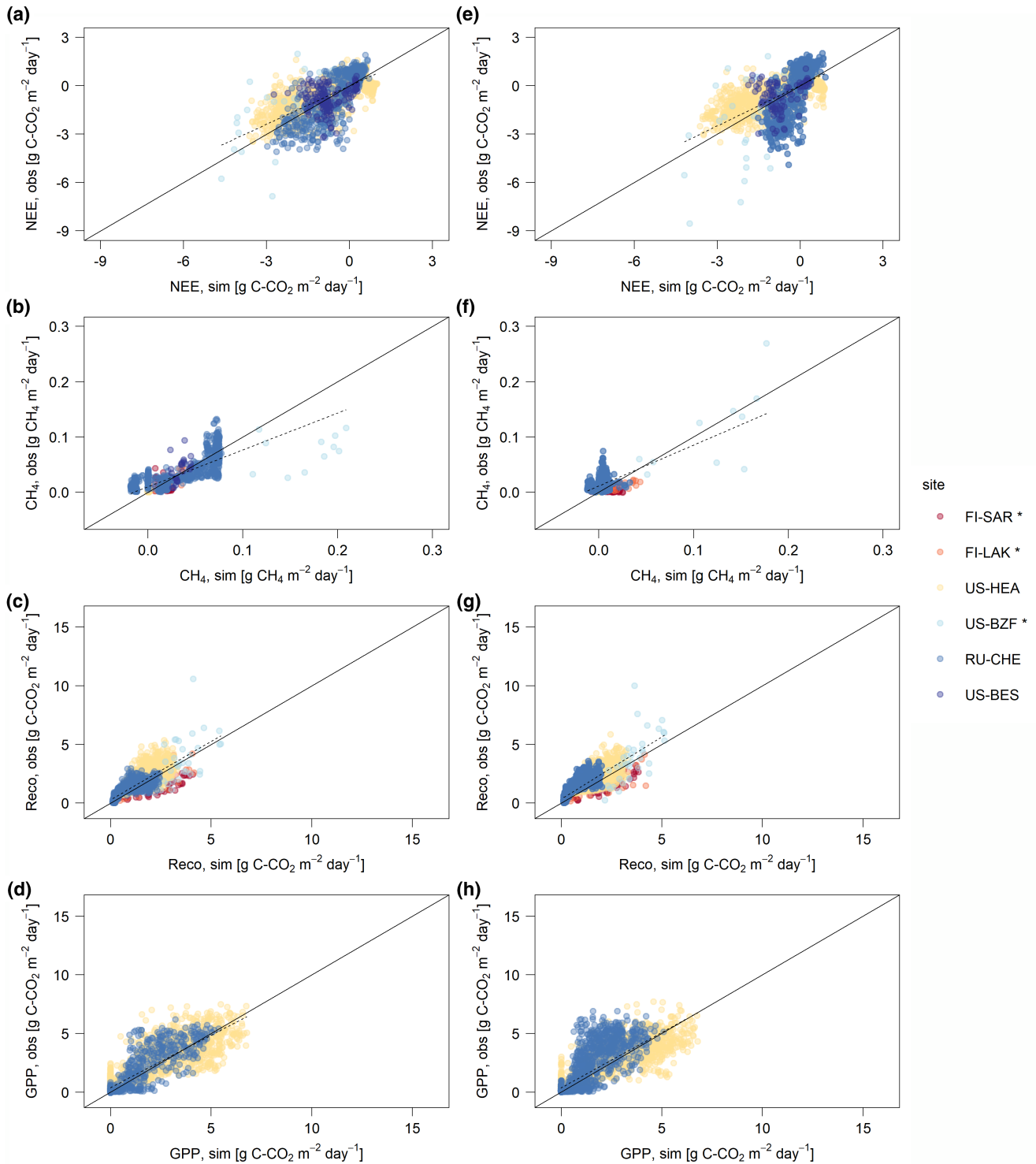


**FIGURE 1** Comparison of NEE (a, e), CH<sub>4</sub> (b, f),  $R_{\text{eco}}$  (c, g), and GPP (d, h) between the model simulations (X-axis) and the observations (Y-axis) for control (a–d) and dry (e–h) treatments after the calibration for each site. Lines are drawn for 1:1 comparisons (solid) and regressions (dashed). Asterisks next to the site name indicate non-permafrost peatlands.

for both NEE (average RMSE: 1.04 g C-CO<sub>2</sub> m<sup>-2</sup> day<sup>-1</sup> and MEF: -0.36, Table S1 and Figures 1, 2 and Figure S3) and CH<sub>4</sub> (average RMSE: 0.03 g CH<sub>4</sub> m<sup>-2</sup> day<sup>-1</sup> and MEF: -8.27, Table S1; Figures 1, 2 and Figure S3) for control and drying treatments (for NEE, average RMSE: 1.20 g C-CO<sub>2</sub> m<sup>-2</sup> day<sup>-1</sup> and MEF: -2.05; for CH<sub>4</sub>, average

RMSE: 0.03 g CH<sub>4</sub> m<sup>-2</sup> day<sup>-1</sup> and MEF: -2.84, Table S1; Figures 1, 2 and Figure S3). The model was calibrated using observations from control treatments, and similar model performance for the drying treatment implies that the model can capture the response of C flux to WT variations well (Tables S1 and S2). Fluxes of some sites

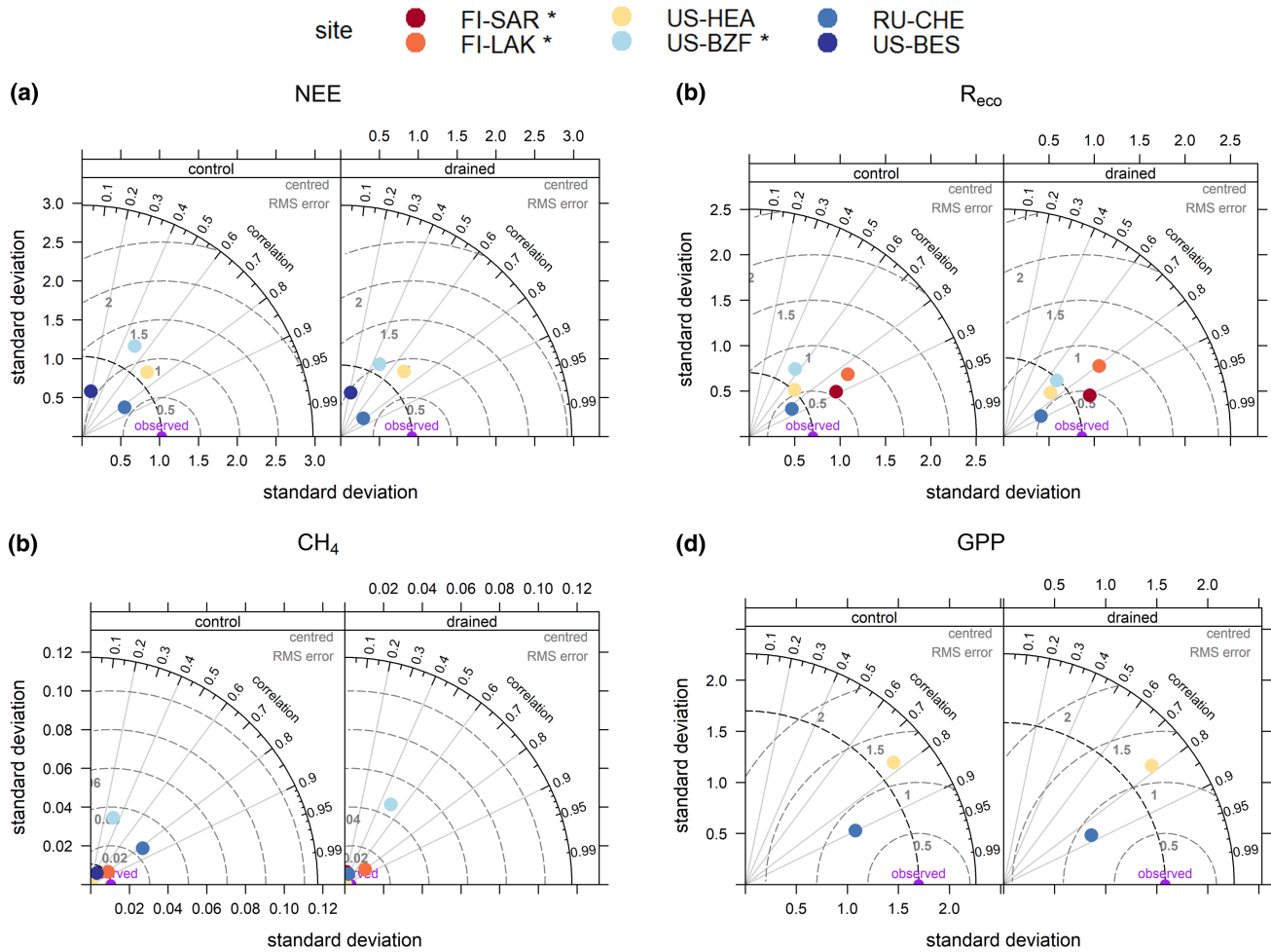


**FIGURE 2** Taylor diagrams of daily NEE (a), CH<sub>4</sub> (b), R<sub>eco</sub> (c), and GPP (d) using model simulations and observations for control and dry treatments. Asterisks next to the site name indicate non-permafrost peatlands.

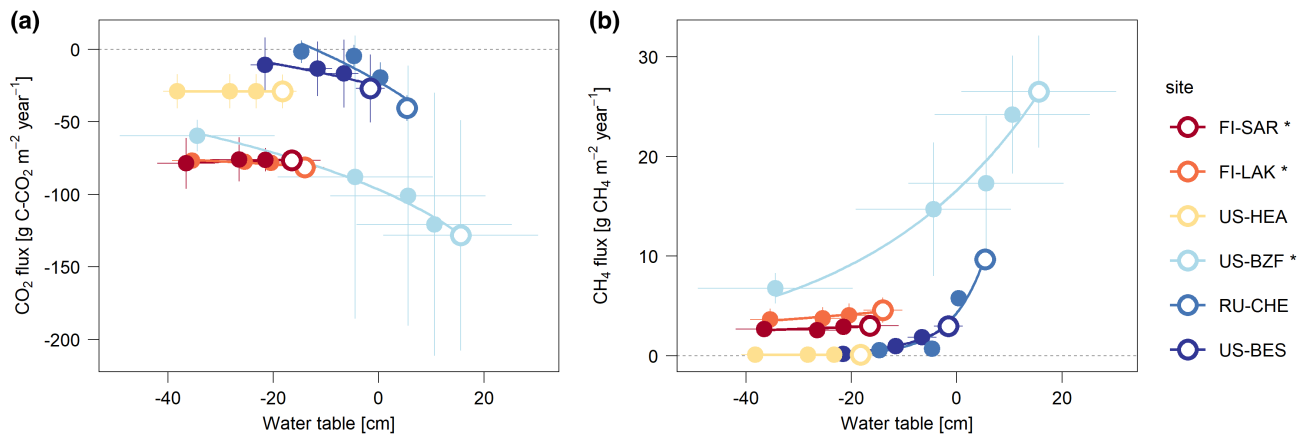


**FIGURE 3** The response of NEE (a) and CH<sub>4</sub> (b) fluxes to sequential drying by 5, 10, 20, and 50 cm (filled circles) starting from the initial WT of control treatment (unfilled circles; highest WT of each site). Points and error bars represent the averages and standard deviations of annual WT and C fluxes for 100-year simulations of each site (color). The exponential lines were fitted for NEE and CH<sub>4</sub>. Positive values of WT denote WT above the soil surface. Asterisks next to the site name indicate non-permafrost peatlands.

showed opposite differences between the simulated and observed dynamics. For example, in the case of US-BZF, drying reduced CH<sub>4</sub> emissions in simulations but the observed data showed increases in

CH<sub>4</sub> emissions. These differences were related to measurements being made at multiple plots with high heterogeneity. Across most sites and fluxes model errors were due to seasonal patterns rather



than magnitude, as inferred from larger LCS than SDSD (Table S1; Figures 1, 2 and Figure S3). The drying treatment (deeper WT) of RU-CHE showed that errors from magnitude were larger than those from the seasonality for CO<sub>2</sub> fluxes, where drying decreased GPP in simulation but increased GPP in observations. With a good agreement between simulations and observations, we described the results based on the simulations from [here](#).

### 3.2 | Response of C fluxes to drying

With the initial WT of the control treatment (simulation during the observation years), NEE ranged from  $-133\text{ g C-CO}_2\text{ m}^{-2}\text{ year}^{-1}$  (US-BZF) to  $-21\text{ g C-CO}_2\text{ m}^{-2}\text{ year}^{-1}$  (US-BES; Figure 5a). Across all sites drying reduced the net CO<sub>2</sub> uptake (i.e., less negative NEE) by  $16\text{ g C-CO}_2\text{ m}^{-2}\text{ year}^{-1}$  on average, with the smallest uptake decrease in US-HEA by  $1\text{ g C-CO}_2\text{ m}^{-2}\text{ year}^{-1}$  (with the smallest drying intensity) and the largest uptake decrease in RU-CHE by  $50\text{ g C-CO}_2\text{ m}^{-2}\text{ year}^{-1}$  (with the largest drying intensity). The change in NEE was driven primarily by reduced GPP ( $11\text{ g C-CO}_2\text{ m}^{-2}\text{ year}^{-1}$  on average) and increased  $R_{\text{eco}}$  ( $5\text{ g C-CO}_2\text{ m}^{-2}\text{ year}^{-1}$  on average). The annual CH<sub>4</sub> emissions were largest at US-BZF ( $19\text{ g C-CH}_4\text{ m}^{-2}\text{ year}^{-1}$ ) and smallest at US-HEA ( $0.1\text{ g C-CH}_4\text{ m}^{-2}\text{ year}^{-1}$ ) for the control treatment (Figure 5b). CH<sub>4</sub> emissions decreased by  $2\text{ g C-CH}_4\text{ m}^{-2}\text{ year}^{-1}$  on average due to the drying treatment, with the smallest decrease in US-HEA by  $0.003\text{ g C-CH}_4\text{ m}^{-2}\text{ year}^{-1}$  and the largest decrease in RU-CHE by  $5\text{ g C-CH}_4\text{ m}^{-2}\text{ year}^{-1}$ .

The drying intensity (change in WT) and the number of years since the start of the drainage differed among sites. To analyze the C flux sensitivity to drying by site, we compared C flux responses to sequential decrease of the WT by 5, 10, 20, and 50 cm compared to the control simulation. As WT draws down, net CO<sub>2</sub> uptake decreased (Figure 3a). This decreased uptake was driven both by reduced GPP and increased  $R_{\text{eco}}$  (Figure S4). The response of NEE to a change of the WT was large when the initial WT was close to the soil surface, and insignificant and almost linear when the initial WT was below 10 cm (Figure 3a and Figure S4). The average decrease in the CO<sub>2</sub> sink was  $13 \pm 15\text{ g C-CO}_2\text{ m}^{-2}\text{ year}^{-1}$  with 10 cm decrease in WT, ranging from 0 to  $36\text{ g C-CO}_2\text{ m}^{-2}\text{ year}^{-1}$ . A similar response was found for CH<sub>4</sub> emissions. They decreased sharply when the initial WT was close to zero cm but showed negligible changes when the initial WT was below 10 cm (Figure 3b and Figure S4). The average decrease in the CH<sub>4</sub> emissions due to 10 cm lower WT cm was  $4 \pm 4\text{ g CH}_4\text{ m}^{-2}\text{ year}^{-1}$  with the range between 0 and  $9\text{ g CH}_4\text{ m}^{-2}\text{ year}^{-1}$ . These responses were mostly driven by reduced CH<sub>4</sub> production and CH<sub>4</sub> transport by plants, while CH<sub>4</sub> oxidation was decreased (US-HEA, RU-CHE, and US-BES), increased (FI-SAR and FI-LAK), or unchanged (US-BZF) with lowered WT (Figure S5).

Permafrost peatlands showed smaller net CO<sub>2</sub> uptake and lower CH<sub>4</sub> emissions compared to the non-permafrost peatlands (Figure 3; note that \* indicates non-permafrost sites), which was also represented by larger and smaller coefficient values of 'a' of the exponential fits for NEE and CH<sub>4</sub>, respectively (Figure S6). Despite smaller

net CO<sub>2</sub> uptake due to drying, the average NEE remained negative during the 100 years of simulation, indicating the persistence of peatland C sinks, even under drier conditions. Two permafrost underlain peatlands (RU-CHE and US-BES), which show low net CO<sub>2</sub> uptake due to the existence of permafrost and large response to drying due to high initial WT, showed net CO<sub>2</sub> emission in some years (Figure 3a), indicating reduced C sinks and the potential switch to C sources.

### 3.3 | Carbon stock changes due to drying

Although CH<sub>4</sub> emissions decreased in response to drying, larger decreases in net CO<sub>2</sub> uptake (less negative NEE) resulted in lower soil C stocks compared to the control (Figure 4a,b). When subjected to a lowered WT by 10 cm, peatlands still accumulate C but the rate of accumulation is lower by  $0.2 \pm 0.2\text{ kg C m}^{-2}$  over 100 years. We found that most of this reduction in C accumulation came from the active (labile) C pool (Figure 4d). Larger decreases in the active C pool and C stock were observed in US-BZF and RU-CHE, where the initial WT is close to 0 and the NEE response to drying was stronger than at other sites (Figure 4a,b). The most significant reduction in C stock (over  $2\text{ kg C m}^{-2}$ ) was observed at US-BZF with 50 cm lower WT, where permafrost does not exist (Figure 4a). Increasing photosynthetic uptake due to drying (increasing  $V_{\text{c,max25}}$  by 10%) reduced the differences in GPP between simulation and observation at US-BZF and RU-CHE, where drying increased GPP (Table S2). Because of the larger C input to soil, increased GPP increased C stock compared to the control treatment in most sites (Figure 4c), out-compensating the C loss by drying. However, it was not the case for US-BZF when dried by >10 cm, that additional C input due to increased productivity was not enough to offset enhanced  $R_{\text{h}}$ .

### 3.4 | Net GHG balance change

When comparing C fluxes between control and a lower WT by 10 cm over 100 years, drying reduced net CO<sub>2</sub> uptake (Figure 5a,d), but decreased CH<sub>4</sub> emissions (Figure 5b,e). These contrasting effects are combined using GWP\*, with the following patterns observed across the study sites: control treatments of US-BZF and RU-CHE acted as net CO<sub>2-eq</sub> sources, FI-SAR, US-HEA, and US-BES as CO<sub>2-eq</sub> sinks, and FI-LAK switched from a CO<sub>2-eq</sub> source to sink after 50 years (Figure 5c). Lowering the WT by 10 cm reduced CO<sub>2-eq</sub> emissions by  $310 \pm 360\text{ g CO}_{2\text{-eq}}\text{ m}^{-2}\text{ year}^{-1}$  because reduced CH<sub>4</sub> emissions played a larger role than the reduced CO<sub>2</sub> uptake (Figure 5f). It is noteworthy that when the initial CH<sub>4</sub> emission rates were high, as in the case of US-BZF, the peatland still acted as a net CO<sub>2-eq</sub> source after drying (Figure 5c). Peatlands that had the initial WT close to the soil surface showed larger responses than those that experienced a lower WT (Figure 5). Similar trends were shown for drying by 5 cm and 20 cm, but we observed smaller reductions in CO<sub>2-eq</sub> emissions with smaller drying intensity (Figure S7).

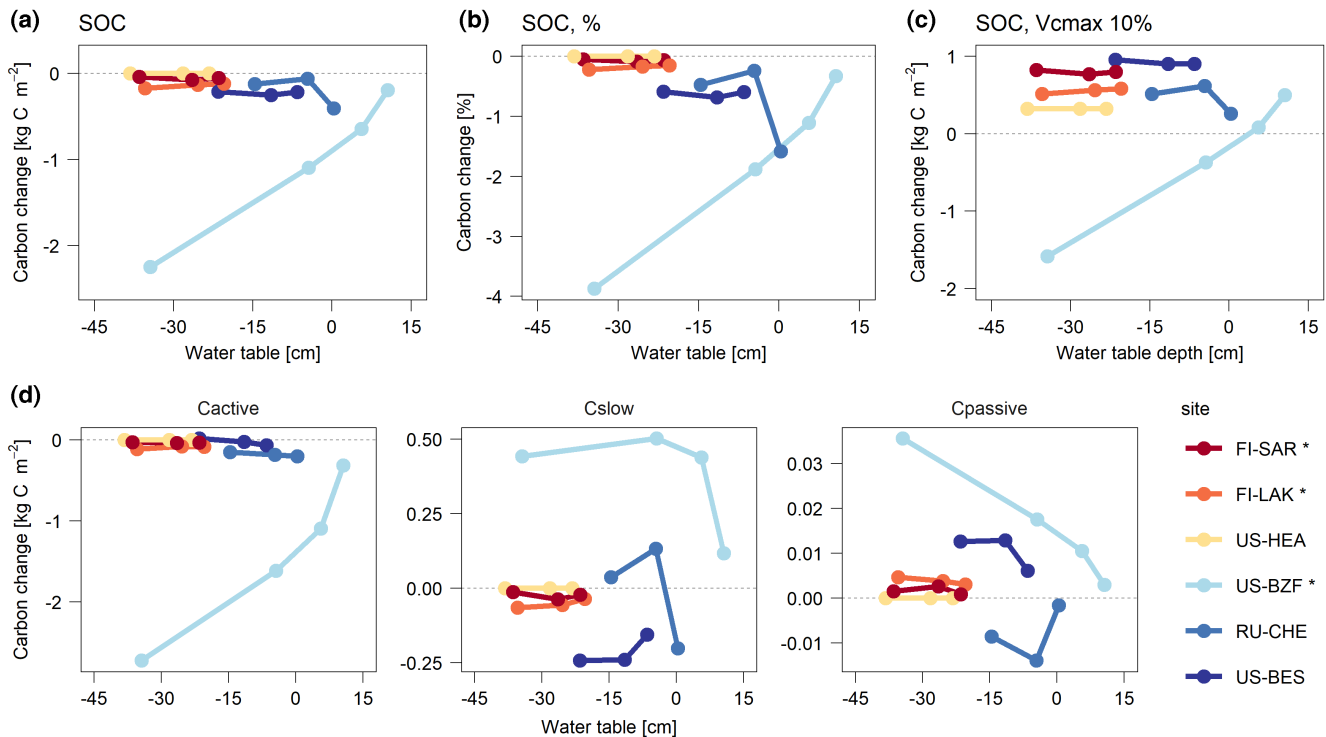


**FIGURE 4** Carbon stock change due to decreasing WT by 5, 10, 20, and 50 cm compared to the control treatment. Total C change (a), total C change in % (b), total C change when  $V_{c_{max25}}$  is increased by 10% (c), and C change by pool (d). Negative (positive) values represent C loss (gain) or smaller (larger) C accumulation compared to the control treatment. Positive values of WT denote WT above the soil surface. Asterisks next to the site name indicate non-permafrost peatlands.

## 4 | DISCUSSION

### 4.1 | Responses of $\text{CO}_2$ and $\text{CH}_4$ fluxes to drying

Carbon sequestration and storage is one of the vital climate regulating services provided by peatlands; however, the C storage capacity of peatlands may be greatly altered under changing climatic conditions. We showed that drying of peatlands by lowering WT resulted in less C sequestration. First, lowered WT decreased C input into soil, due to reduced photosynthetic activity (i.e., GPP) under decreased water availability in shallow soil layers, where most roots exist. This response can be, however, different depending upon plant species. For example, vascular plants show higher productivity with lowered WT, while mosses show lower productivity (Sulman et al., 2010). In addition to the instant responses of GPP to WT variations, plant composition can shift (Breeuwer et al., 2009; Potvin et al., 2015) and GPP may decrease (Churchill et al., 2014; McPartland et al., 2019) or increase (Kittler et al., 2016) when WT in peatlands persistently lowers. Increasing productivity due to drying can compensate the C loss, but may not be enough under intense drying as shown in Figure 4c.

In addition to reduced photosynthesis, peatland drying generally increased peat C loss through heterotrophic respiration ( $R_h$ ) despite decreased autotrophic respiration ( $R_a$ ) offsetting this change. Respiration rates are higher under aerobic conditions

compared to water-saturated conditions (Moyano et al., 2013), and this mechanistic relationship is well represented in the model. Although drying did not significantly affect soil temperatures in the simulation, drying reduced deep soil temperature at US-HEA and RU-CHE in the observations because of insulation effects of drier peat at the surface (Kwon et al., 2019). This implies that the respiration response of deep soil layers to drying can be limited as compared to the surface soil layers. The combined effects of drying on GPP and  $R_{eco}$ , thus the direction of C gain or loss, are largely dependent on the response of the plant productivity to drying, as shown in the reversed C stock change with the increased productivity in most sites (Figure 4a,c). The initial WT also plays a role that higher initial WT with a large proportion of labile C can show a stronger  $R_h$  response to drying, driving the net  $\text{CO}_2$  response toward a larger loss.

In contrast to the reduced net  $\text{CO}_2$  uptake following peatland drying,  $\text{CH}_4$  emissions decreased with lowered WT with similar decreasing rates to those of the previous studies (Evans et al., 2021; Huang et al., 2021; Kuhn et al., 2021; Nykänen et al., 1998; Olefeldt et al., 2013). This exponential decrease with lower WT (Figure 3b) can be attributed to thinner anaerobic peat layers at deep soil layers and thicker aerobic peat layers at the surface (Kuhn et al., 2021; Kwon et al., 2017; Olefeldt et al., 2013). Although atmospheric  $\text{CH}_4$  can be oxidized in top soils by high-affinity methanotrophs, thereby reducing net  $\text{CH}_4$  emission to the atmosphere (Oh et al., 2020), the response of  $\text{CH}_4$  emissions

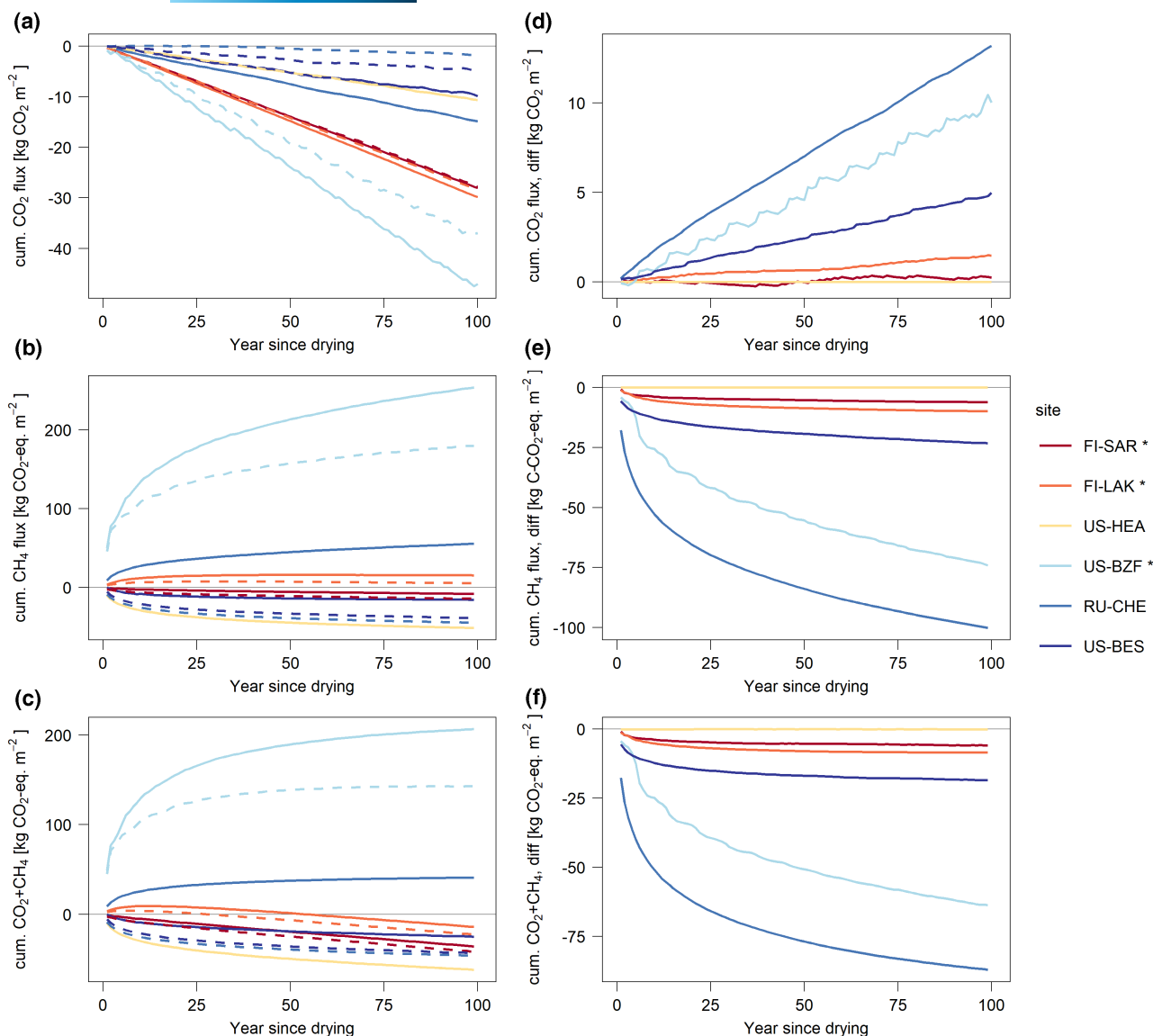


**FIGURE 5** Cumulative CO<sub>2</sub> (a), CH<sub>4</sub> (b), and combined (c) flux change over 100 years for control (solid) and dry by 10 cm (dashed) treatments. Positive (negative) values represent net emission (uptake) to (from) the atmosphere (a–c). The differences between control and dry by 10 cm treatments are depicted in d–f, with positive values representing increased CO<sub>2</sub>-eq emissions or decreased CO<sub>2</sub>-eq uptake compared to the control treatment. Asterisks next to the site name indicate non-permafrost peatlands.

to WT was largely driven by CH<sub>4</sub> production because most CH<sub>4</sub> is oxidized by low-affinity methanotrophs when abundant CH<sub>4</sub> exists in peat soils (Kwon et al., 2017, 2021). The initial WT, thus, largely affected CH<sub>4</sub> emissions through the rate of methanogenesis (aerobic respiration to methanogenesis ratio;  $k$ ) and methanotrophy ( $k_{MT}$ ; turnover time of methanotrophy; Figure S8). For example, a low ratio of aerobic respiration to methanogenesis (smaller  $k$ ; higher CH<sub>4</sub> production potential) in RU-CHE and US-BES compared to other sites can be attributed to higher average WT and smaller temporal variations (Figure S1), which kept the soil more anaerobic than other sites. The variations in these optimized parameters among sites may represent other environmental status that the model does not include, such as substrate status (Chang et al., 2020; Roy Chowdhury et al., 2021).

## 4.2 | Variations in sensitivity to drying

The fluxes of CO<sub>2</sub> and CH<sub>4</sub> were sensitive to drying when the initial WT was close to 0. Unless there had been an abrupt hydrological change before the observations, the current WT can be represented as the long-term WT. Water-saturated peatlands, which are less exposed to aerobic conditions, have a large fraction of partially decomposed C in the topsoil compared to peatlands with lower WT, the topsoil of which has already been largely decomposed. Thus, a large fraction of remaining labile C can be rapidly decomposed to CO<sub>2</sub> instead of CH<sub>4</sub> when WT lowers, thus showing a stronger drying response. Non-permafrost peatland with high initial WT in US-BZF showed the strongest response to drying up to 50 cm, with >2 kg C m<sup>-2</sup> less C accumulating over

100 years compared to the initial WT condition. In contrast, peatlands with low initial WT may show no or subtle responses to drying due to less available labile C in deeper soil layers (Huang et al., 2021; Muhr et al., 2011). Larger temperature fluctuations in shallow layers compared to deeper layers may contribute to these stronger responses (Kwon et al., 2017). Fluctuations in WT can also affect the magnitude of the responses: Although the largest response was observed in US-BZF because of the combination of high WT and a large C stock, temporal lowering of WT resulted in a smaller slope change than in RU-CHE (Figure 3 and Figure S6), where WT was constantly high.

Permafrost underlain peatlands showed lower CO<sub>2</sub> and CH<sub>4</sub> fluxes compared to the other sites, as shown in previous studies (Kuhn et al., 2021; Olefeldt et al., 2013; Treat et al., 2018). This is mainly because permafrost limits the plant rooting depth and productivity, subsequently leading to reduced C input to soils, and reduced decomposition. However, the responses to drying in terms of direction and magnitude were similar between permafrost and non-permafrost peatlands. Low absolute C fluxes in permafrost peatlands affected the variations, leading to almost no response in C fluxes and stock to drying in US-HEA, where initial WT is low and the existence of permafrost retards deep soil processes. Furthermore, low absolute CO<sub>2</sub> fluxes in RU-CHE and US-BES resulted in a temporal switch from net CO<sub>2</sub> uptake to net CO<sub>2</sub> emission in response to drying.

The simulated exponential decrease in CH<sub>4</sub> fluxes as a function of WT was very similar to previous observations in natural (Huang et al., 2021; Kuhn et al., 2021; Nykänen et al., 1998; Olefeldt et al., 2013) and managed peatlands (Evans et al., 2021). However, our simulations showed exponentially decreasing NEE to near-neutral NEE with lowered WT, in contrast to the linear relationship between WT and NEE in the managed peatlands of Evans et al. (2021). The difference can be attributed to the management (harvest): Fens and bogs without harvest hardly showed the net CO<sub>2</sub> emissions with low WT, but grasslands and croplands showed net CO<sub>2</sub> emissions with low WT possibly because of different biogeochemical processes from natural peatlands, for example, disturbance and nutrient status (Evans et al., 2021). Nevertheless, we can further investigate whether natural peatlands can act as the net CO<sub>2</sub> source with extremely low WT by including more sites and more years with climate variability (Fenner & Freeman, 2011; Qiu et al., 2022).

### 4.3 | C stock change and warming effects

Stronger decreases in the net CO<sub>2</sub> uptake than decreases in CH<sub>4</sub> emission resulted in smaller C accumulation in dry peatlands. Also, water-saturated peatlands were more vulnerable to C loss in response to drying compared to peatlands with initially lower WT. Furthermore, a significant C loss was observed in non-permafrost peatlands and a possible switch from C sink to source in permafrost peatlands. It is challenging to detect the change in SOC in field manipulation experiments since the soil C pool changes slowly, but we can infer from a large accumulation of C in peatlands that wet

conditions are favorable for slower turnover and higher C accumulation in soils (Hugelius et al., 2020; MacDonald et al., 2006). Whether these C sinks become C sources or not is highly uncertain, but it is likely that C sink capacity decreases or even turns into a C source (Hugelius et al., 2020), combined with higher risk of peat fire may make these C stocks more vulnerable to future warming (Turetsky et al., 2011; Witze, 2020). Günther et al. (2020) showed that peatland drying has a net warming effect due to larger increases in long-lived CO<sub>2</sub> emission than decreases in short-lived CH<sub>4</sub> emission, which contrasts with this present study. Günther et al. (2020) used emission factors to estimate warming effects, with much larger CO<sub>2</sub> emission rates than CH<sub>4</sub> in temperate and tropical zones compared to the smaller warming effects reported here for the drying response of boreal peatlands. As both CO<sub>2</sub> and CH<sub>4</sub> fluxes are responding non-linearly to a lower WT and the relative changes between CO<sub>2</sub> and CH<sub>4</sub> fluxes differ by site combined with temperature sensitivity (Chen et al., 2021), more thorough analyses are needed to quantify the compound effects of warming and drying on peatland C.

We did not include climate change other than WT drawdown in this study, but WT dynamics are tightly connected with climate change. For example, warming itself can increase evapotranspiration and warming-induced increases in plant biomass can accelerate this change (Helbig et al., 2020), further lowering WT in peatlands. In addition, drier peatlands with lower water availability can increase sensible heat flux, which can warm lower atmosphere (Göckede et al., 2017). Changing precipitation patterns can modify WT of peatlands in the local and regional scales (Qiu et al., 2022). Because of high uncertainty and large temporal and spatial variations in the relationship among temperature, precipitation, and peatland WT, it is challenging to forecast the direction and magnitude of C response of northern peatlands and their feedback with climate. However, studies including climate change predict that northern peatlands will reduce their C sink capacity (Chaudhary et al., 2020) or lose C (Treat et al., 2021; Wu et al., 2013) especially under strong warming scenarios (Chaudhary et al., 2022; Qiu et al., 2022). Although the magnitude of C loss in response to WT changes in our study is less than the previously studied temperature and precipitation responses, our results indicate that drying may exacerbate C loss due warming of northern peatlands.

### 4.4 | Limitations and future directions

Despite well simulated fluxes after optimizing the model parameters, some processes can be added for further improvement. For example, our model does not differentiate peatland types, such as fens and bogs, which have distinguishable hydrologic connectivity to groundwater and nutrient supply (Charman, 2009). Greater parameter value ( $V_{c_{max25}}$ ) for plant productivity in US-BZF (fen) than other sites could have represented higher nutrient supply, but different seasonality among peatland types may not be captured depending on the relative importance of hydrologic connectivity on the C cycle. Furthermore, processes in the standing water in fens, such as CH<sub>4</sub>

oxidation in the water column (Ward et al., 2020), contribution of algae (Kane et al., 2021) and predation (Wyatt et al., 2021), can be incorporated.

Our current model has one peatland-representative plant functional type and does not distinguish multiple peatland plant species, such as sedges, mosses, shrubs, and trees, which can respond differently to short-term hydrological changes (Sulman et al., 2010), and their potential compositional change following long-term hydrological changes (Breeuwer et al., 2009). We did not include peatland forestry in this study, but intensive drainage that results in significant tree growth can be another aspect to consider, which may increase (Krüger et al., 2016; Minkkinen et al., 1999; Simola et al., 2012) or decrease (Krüger et al., 2016; Minkkinen et al., 1999; Nykänen et al., 2020; Simola et al., 2012) soil C but increase plant biomass and total terrestrial C stock (Minkkinen et al., 1999). Furthermore, potentially deepening rooting depth (priming effects) may accelerate C loss as well in deeper soils (Keuper et al., 2020). In addition, our current model has constant peatland surface elevation, although peatland surfaces are not static and changes in their physical properties can alter soil biogeochemical properties: Persistent dry conditions can change the peat properties, such as bulk density, which can subsequently influence hydraulic and thermal properties, decomposition rates, and plant composition (Kreyling et al., 2021; Nykänen et al., 1998; Turetsky et al., 2014). After a substantial portion of the dry peat at the surface is decomposed and becomes compact, the surface subsides and the relative WT becomes higher (hydrological self-regulation of peatlands; Belyea & Baird, 2006; Dise, 2009; Waddington et al., 2015). We prescribed the WT with the observations (relative to the surface), and short-term responses up to the observation point were well simulated. However, without dynamic surface elevation (e.g., subsidence) represented in the current model, WT drawdown and its effect on the C cycle can be overestimated in the long-term especially in non-permafrost peatlands (Nijp et al., 2017). This overestimation can be less of a concern in permafrost peatlands, because permafrost and ground ice block or retard the vertical and lateral water drainage, and permafrost thaw and ground ice melt will remove surface water that connects the hydrological feedback process. The intensity of this change can be also species specific and can be strong at the surface, where abundant macro-pores exist (McCarter et al., 2020). Additional model development to take into account these short term and long term as well as aboveground and belowground factors could further reduce the uncertainty of the direction and magnitude of C stock changes.

With a finely calibrated land surface model with a multilayer soil module, we demonstrated decreasing CO<sub>2</sub> sink strength and CH<sub>4</sub> emissions in response to drying, and these responses were stronger when initial WT conditions were close to the soil surface. There is limitation in upscaling this response to the whole northern peatlands based on the results from only six northern peatlands. For example, US-BZF showed the highest CH<sub>4</sub> fluxes among all six sites of this study, but its CH<sub>4</sub> flux rate is comparably

lower than other northern peatlands (Kuhn et al., 2021) possibly because methanogens are outcompeted by reducers of alternative electron acceptors (Kane et al., 2013; Rupp et al., 2021). Variations in parameters that are associated with methanogenesis (*k*) partially represent redox status, yet such processes can be included. Using averaged parameters for the whole region can over- or under-estimate fluxes (Qiu et al., 2018; Salmon et al., 2021; Treat et al., 2018), or converge to the average fluxes. In addition, despite several available peatland/wetland maps (Hugelius et al., 2020; Olefeldt et al., 2021; Xu et al., 2018) and possible usage of precipitation minus evapotranspiration as a proxy of relative WT variations (Gulev et al., 2021), the lack of highly heterogeneous local WT data in the northern peatlands will not allow us to accurately assess the current responses of northern peatlands to changes in water balance. In addition to the high uncertainty in the temporal and spatial variations in WT depending on climate and anthropogenic activities, permafrost-thaw-related changes add more complexity to evaluation of long-term trends. When excessive ground ice melts, it can induce further hydrological changes (Andresen et al., 2020; Lewis et al., 2012; Nitzbon et al., 2020; Rodenhizer et al., 2020). Thus, the inclusion of ground ice dynamics and the associated topographical and hydrological change in the model are essential to constrain C flux and stock change in permafrost peatlands (Cai et al., 2020; O'Neill et al., 2019).

Although peatland drying reduced the net CO<sub>2-eq</sub> fluxes, it decreased C accumulation, which is one of the crucial functions of northern peatlands. In particular, peatlands with a high WT are more vulnerable to C loss, including a large potential C loss in non-permafrost peatlands and a possible switch from C sink to source in permafrost peatlands. Human-induced drainage can be avoided to reduce this C loss, but climate-driven peatland drying, including permafrost-thaw related drying, cannot be prevented without strong climate change mitigation. Furthermore, re-wetting does not necessarily restore peatlands to pre-drying conditions (Harris et al., 2020; Kreyling et al., 2021), and the intact wet conditions are critical for maximizing C storing function of peatlands.

## ACKNOWLEDGMENTS

This research was supported by the l'Agence Nationale de la Recherche (Make Our Planet Great Again; ANR-18-MPGA-0007). Chunjing Qiu has been supported by the ANR (CLAND Convergence Institute; ANR-16-CONV-0003). Elodie Salmon has been supported by Horizon 2020 (CRESCENDO grant no. 641816), and Labex VOLTAIRE (ANR-10-LABX-100-01). Bertrand Guenet has been supported by the grant (Holistic management practices, modelling and monitoring for European forest soils [H2020 grant agreement No. 101000289]). Eugénie S. Euskirchen acknowledges funding provided by the US Geological Survey, Research Work Order 224 to the University of Alaska Fairbanks, the Bonanza Creek Long-Term Ecological Research Program funded by the National Science Foundation (NSF DEB-1026415, DEB-1636476) and the NSF Long-Term Research in Environmental



Biology Program (NSF LTREB 2011276). Hannu Nykänen acknowledges Atmosphere and Climate Competence Center (Academy of Finland; 337550).

## CONFLICT OF INTEREST

The authors declare no conflicts of interest.

## DATA AVAILABILITY STATEMENT

All the model simulation data are stored at [zenodo.org \(10.5281/zenodo.6817633\)](https://zenodo.org/doi/10.5281/zenodo.6817633). Observation data used for the model optimization is available as follows: (1) FI-SAR & FI-LAK: <https://doi.org/10.5281/zenodo.6967198>, (2) US-BZF: <https://doi.org/10.17190/AMF/1756433>, (3) US-HEA: <https://doi.org/10.6073/pasta/34c20956a48edb4507add832b98a7fa6> and <https://doi.org/10.6073/pasta/2959f51f79d067ce01d2c74a8d5fbb75>, (4) RU-CHE: <https://doi.org/10.18140/FLX/1669654> and <https://doi.org/10.18140/FLX/1669655>, and (5) US-BES: <https://doi.org/10.18739/A20Z70Z1H>.

## ORCID

Min Jung Kwon  <https://orcid.org/0000-0002-7330-2320>  
 Ashley Ballantyne  <https://orcid.org/0000-0003-1532-5126>  
 Philippe Ciais  <https://orcid.org/0000-0001-8560-4943>  
 Chunjing Qiu  <https://orcid.org/0000-0002-9951-3951>  
 Elodie Salmon  <https://orcid.org/0000-0001-5066-4591>  
 Nina Raoult  <https://orcid.org/0000-0003-2907-9456>  
 Bertrand Guenet  <https://orcid.org/0000-0002-4311-8645>  
 Mathias Göckede  <https://orcid.org/0000-0003-2833-8401>  
 Eugénie S. Euskirchen  <https://orcid.org/0000-0002-0848-4295>  
 Hannu Nykänen  <https://orcid.org/0000-0002-1410-9352>  
 Edward A. G. Schuur  <https://orcid.org/0000-0002-1096-2436>  
 Catherine M. Dieleman  <https://orcid.org/0000-0002-4280-5849>

## REFERENCES

- Allen, M. R., Shine, K. P., Fuglestedt, J. S., Millar, R. J., Cain, M., Frame, D. J., & Macey, A. H. (2018). A solution to the misrepresentations of CO<sub>2</sub>-equivalent emissions of short-lived climate pollutants under ambitious mitigation. *NPJ Climate and Atmospheric Science*, 1(1), 1–8. <https://doi.org/10.1038/s41612-018-0026-8>
- Andresen, C. G., Lawrence, D. M., Wilson, C. J., McGuire, A. D., Koven, C., Schaefer, K., Jafarov, E., Peng, S., Chen, X., Gouttevin, I., Burke, E., Chadburn, S., Ji, D., Chen, G., Hayes, D., & Zhang, W. (2020). Soil moisture and hydrology projections of the permafrost region—A model intercomparison. *The Cryosphere*, 14(2), 445–459. <https://doi.org/10.5194/tc-14-445-2020>
- Atanasiu, L. (1971). Photosynthesis and respiration of three mosses at winter low temperatures. *Bryologist*, 74(1), 23–27. <https://doi.org/10.2307/3241751>
- Avis, C. A., Weaver, A. J., & Meissner, K. J. (2011). Reduction in areal extent of high-latitude wetlands in response to permafrost thaw. *Nature Geoscience*, 4, 444–448. <https://doi.org/10.1038/ngeo1160>
- Baird, A. J., Beckwith, C. W., Waldron, S., & Waddington, J. M. (2004). Ebullition of methane-containing gas bubbles from near-surface *Sphagnum peat*. *Geophysical Research Letters*, 31(21), L21505. <https://doi.org/10.1029/2004GL021157>
- Bastrikov, V., MacBean, N., Bacour, C., Santaren, D., Kuppel, S., & Peylin, P. (2018). Land surface model parameter optimisation using in situ flux data: Comparison of gradient-based versus random search algorithms (a case study using ORCHIDEE v1.9.5.2). *Geoscientific Model Development*, 11(12), 4739–4754. <https://doi.org/10.5194/gmd-11-4739-2018>
- Belyea, L. R., & Baird, A. J. (2006). Beyond “the limits to peat bog growth”: Cross-scale feedback in peatland development. *Ecological Monographs*, 76(3), 299–322. [https://doi.org/10.1890/0012-9615\(2006\)076\[0299:BTLPB\]2.0.CO;2](https://doi.org/10.1890/0012-9615(2006)076[0299:BTLPB]2.0.CO;2)
- Bintanja, R., & Andry, O. (2017). Towards a rain-dominated Arctic. *Nature Climate Change*, 7, 263–267. <https://doi.org/10.1038/nclimate3240>
- Bintanja, R., & Selten, F. M. (2014). Future increases in Arctic precipitation linked to local evaporation and sea-ice retreat. *Nature*, 509, 479–482. <https://doi.org/10.1038/nature13259>
- Botta, A., Viovy, N., Ciais, P., Friedlingstein, P., & Monfray, P. (2000). A global prognostic scheme of leaf onset using satellite data. *Global Change Biology*, 6(7), 709–725. <https://doi.org/10.1046/j.1365-2486.2000.00362.x>
- Breuer, A., Robroek, B. J. M., Limpens, J., Heijmans, M. M. P. D., Schouten, M. G. C., & Berendse, F. (2009). Decreased summer water table depth affects peatland vegetation. *Basic and Applied Ecology*, 10(4), 330–339. <https://doi.org/10.1016/j.baae.2008.05.005>
- Bridgman, S. D., Megonigal, J. P., Keller, J. K., Bliss, N. B., & Trettin, C. (2006). The carbon balance of North American wetlands. *Wetlands*, 26(4), 889–916. [https://doi.org/10.1672/0277-5212\(2006\)26\[889:TCBONA\]2.0.CO;2](https://doi.org/10.1672/0277-5212(2006)26[889:TCBONA]2.0.CO;2)
- Byrne, K., Chojnicki, B., Christensen, T., Drosler, M., Frohling, S., Lindroth, A., Mailhammer, J., Malmer, N., Selin, P., Turunen, J., Valentini, R., & Zetterberg, L. (2004). EU peatlands: Current carbon stocks and trace gas fluxes, Report 4/2004 to ‘Concerted action: Synthesis of the European Greenhouse Gas Budget’, Geosphere-Biosphere Centre, University of Lund, Sweden. [https://scholars.unh.edu/earthsci\\_facpub/490](https://scholars.unh.edu/earthsci_facpub/490)
- Cai, L., Lee, H., Aas, K. S., & Westermann, S. (2020). Projecting circum-Arctic excess ground ice melt with a sub-grid representation in the Community Land Model. *The Cryosphere Discussions*, 14(12), 1–28. <https://doi.org/10.5194/tc-2020-91>
- Cain, M., Lynch, J., Allen, M. R., Fuglestedt, J. S., Frame, D. J., & Macey, A. H. (2019). Improved calculation of warming-equivalent emissions for short-lived climate pollutants. *NPJ Climate and Atmospheric Science*, 2(1), 1–7. <https://doi.org/10.1038/s41612-019-0086-4>
- Chang, K.-Y., Riley, W. J., Crill, P. M., Grant, R. F., & Saleska, S. R. (2020). Hysteretic temperature sensitivity of wetland CH<sub>4</sub> fluxes explained by substrate availability and microbial activity. *Biogeosciences*, 17(22), 5849–5860. <https://doi.org/10.5194/bg-17-5849-2020>
- Charman, D. J. (2009). Peat and peatlands. In G. E. Likens (Ed.), *Encyclopedia of Inland Waters* (pp. 541–548). Academic Press. <https://doi.org/10.1016/B978-012370626-3.00061-2>
- Chaudhary, N., Westermann, S., Lamba, S., Shurpali, N., Sannel, A. B. K., Schurgers, G., Miller, P. A., & Smith, B. (2020). Modelling past and future peatland carbon dynamics across the pan-Arctic. *Global Change Biology*, 26(7), 4119–4133. <https://doi.org/10.1111/gcb.15099>
- Chaudhary, N., Zhang, W., Lamba, S., & Westermann, S. (2022). Modeling pan-Arctic peatland carbon dynamics under alternative warming scenarios. *Geophysical Research Letters*, 49(10), e2021GL095276. <https://doi.org/10.1029/2021GL095276>
- Chen, H., Xu, X., Fang, C., Li, B., & Nie, M. (2021). Differences in the temperature dependence of wetland CO<sub>2</sub> and CH<sub>4</sub> emissions vary with water table depth. *Nature Climate Change*, 11(9), 766–771. <https://doi.org/10.1038/s41558-021-01108-4>
- Churchill, A. C., Turetsky, M. R., McGuire, D. A., & Hollingsworth, T. N. (2014). Response of plant community structure and primary productivity to experimental drought and flooding in an Alaskan fen1. *Canadian Journal of Forest Research*, 45, 185–193. <https://doi.org/10.1139/cjfr-2014-0100>
- Dise, N. B. (2009). Peatland response to global change. *Science*, 326(5954), 810–811. <https://doi.org/10.1126/science.1174268>



- Douville, H., Raghavan, K., Renwick, J., Allan, R. P., Arias, P. A., Barlow, M., Cerezo-Mota, R., Cherchi, A., Gan, T. Y., Gergis, J., Jiang, D., Khan, A., Mba, W. P., Rosenfeld, D., Tierney, J., & Zolina, O. (2021). Water cycle changes. In *Climate Change 2021: The physical science bases. Contribution of Working Group I to the sixth assessment report of the Intergovernmental Panel on Climate Change*. Cambridge University Press.
- Ekici, A., Beer, C., Hagemann, S., Boike, J., Langer, M., & Hauck, C. (2014). Simulating high-latitude permafrost regions by the JSBACH terrestrial ecosystem model. *Geoscientific Model Development*, 7(2), 631–647. <https://doi.org/10.5194/gmd-7-631-2014>
- Euskirchen, E. S., Kane, E. S., Edgar, C. W., & Turetsky, M. R. (2020). When the source of flooding matters: Divergent responses in carbon fluxes in an Alaskan rich fen to two types of inundation. *Ecosystems*, 23(6), 1138–1153. <https://doi.org/10.1007/s10021-019-00460-z>
- Evans, C. D., Peacock, M., Baird, A. J., Artz, R. R. E., Burden, A., Callaghan, N., Chapman, P. J., Cooper, H. M., Coyle, M., Craig, E., Cumming, A., Dixon, S., Gauci, V., Grayson, R. P., Helfter, C., Heppell, C. M., Holden, J., Jones, D. L., Kaduk, J., ... Morrison, R. (2021). Overriding water table control on managed peatland greenhouse gas emissions. *Nature*, 593(7860), 548–552. <https://doi.org/10.1038/s41586-021-03523-1>
- Fenner, N., & Freeman, C. (2011). Drought-induced carbon loss in peatlands. *Nature Geoscience*, 4(12), 895–900. <https://doi.org/10.1038/ngeo1323>
- Fewster, R. E., Morris, P. J., Ivanovic, R. F., Swindles, G. T., Peregon, A. M., & Smith, C. J. (2022). Imminent loss of climate space for permafrost peatlands in Europe and Western Siberia. *Nature Climate Change*, 12(4), 373–379. <https://doi.org/10.1038/s41558-022-01296-7>
- Göckede, M., Kittler, F., Kwon, M. J., Burjack, I., Heimann, M., Kolle, O., Zimov, N., & Zimov, S. (2017). Shifted energy fluxes, increased Bowen ratios, and reduced thaw depths linked with drainage-induced changes in permafrost ecosystem structure. *The Cryosphere*, 11(6), 2975–2996. <https://doi.org/10.5194/tc-11-2975-2017>
- Göckede, M., Kwon, M. J., Kittler, F., Heimann, M., Zimov, N., & Zimov, S. (2019). Negative feedback processes following drainage slow down permafrost degradation. *Global Change Biology*, 25(10), 3254–3266. <https://doi.org/10.1111/gcb.14744>
- Goldberg, D. E., & Holland, J. H. (1988). Genetic algorithms and machine learning. *Machine Learning*, 3(2), 95–99. <https://doi.org/10.1023/A:1022602019183>
- Gorham, E. (1991). Northern peatlands: Role in the carbon cycle and probable responses to climatic warming. *Ecological Applications*, 1(2), 182–195. <https://doi.org/10.2307/1941811>
- Gornall, J., Jónsdóttir, I., Woodin, S., & van der Wal, R. (2007). Arctic mosses govern belowground environment and ecosystem processes. *Oecologia*, 153, 931–941. <https://doi.org/10.1007/s00442-007-0785-0>
- Greve, P., Orłowsky, B., Mueller, B., Sheffield, J., Reichstein, M., & Seneviratne, S. I. (2014). Global assessment of trends in wetting and drying over land. *Nature Geoscience*, 7(10), 716–721. <https://doi.org/10.1038/ngeo2247>
- Guimberteau, M., Zhu, D., Maignan, F., Huang, Y., Yue, C., Dantec-Nédélec, S., Otlé, C., Jorner-Puig, A., Bastos, A., Laurent, P., Goll, D., Bowring, S., Chang, J., Guenet, B., Tifafi, M., Peng, S., Krinner, G., Ducharne, A., Wang, F., ... Ciais, P. (2018). ORCHIDEE-MICT (v8.4.1), a land surface model for the high latitudes: Model description and validation. *Geoscientific Model Development*, 11(1), 121–163. <https://doi.org/10.5194/gmd-11-121-2018>
- Gulev, S. K., Thorne, P. W., Ahn, J., Dentener, F. J., Domingues, C. M., Gerland, S., Gong, D., Kaufman, D. S., Nnamchi, H. C., Quaas, J., Rivera, J. A., Sathyendranath, S., Smith, S. L., Trewin, B., von Shuckmann, K., & Vose, R. S. (2021). Changing state of the climate system. In *Climate Change 2021: The physical science bases. Contribution of Working Group I to the sixth assessment report of the intergovernmental panel on climate change*. Cambridge University Press.
- Günther, A., Barthelmes, A., Huth, V., Joosten, H., Jurasinski, G., Koebisch, F., & Couwenberg, J. (2020). Prompt rewetting of drained peatlands reduces climate warming despite methane emissions. *Nature Communications*, 11(1), 1644. <https://doi.org/10.1038/s41467-020-15499-z>
- Harris, L. I., Roulet, N. T., & Moore, T. R. (2020). Drainage reduces the resilience of a boreal peatland. *Environmental Research Communications*, 2(6), 065001. <https://doi.org/10.1088/2515-7620/ab9895>
- Haupt, R. L., & Haupt, S. E. (2004). *Practical genetic algorithms* (2nd ed.). John Wiley & Sons. <https://onlinelibrary.wiley.com/doi/book/10.1002/0471671714>
- Helbig, M., Waddington, J. M., Alekseychik, P., Amiro, B. D., Aurela, M., Barr, A. G., Black, T. A., Blanken, P. D., Carey, S. K., Chen, J., Chi, J., Desai, A. R., Dunn, A., Euskirchen, E. S., Flanagan, L. B., Forbrich, I., Friborg, T., Grelle, A., Harder, S., ... Zyrjanov, V. (2020). Increasing contribution of peatlands to boreal evapotranspiration in a warming climate. *Nature Climate Change*, 10(6), 555–560. <https://doi.org/10.1038/s41558-020-0763-7>
- Huang, Y., Ciais, P., Luo, Y., Zhu, D., Wang, Y., Qiu, C., Goll, D. S., Guenet, B., Makowski, D., De Graaf, I., Leifeld, J., Kwon, M. J., Hu, J., & Qu, L. (2021). Tradeoff of CO<sub>2</sub> and CH<sub>4</sub> emissions from global peatlands under water-table drawdown. *Nature Climate Change*, 11(7), 618–622. <https://doi.org/10.1038/s41558-021-01059-w>
- Hugelius, G., Loisel, J., Chadburn, S. E., Jackson, R. B., Jones, M., MacDonald, G., Marushchak, M., Olefeldt, D., Packalen, M., Siewert, M. B., Treat, C., Turetsky, M., Voigt, C., & Yu, Z. (2020). Large stocks of peatland carbon and nitrogen are vulnerable to permafrost thaw. *Proceedings of the National Academy of Sciences of the United States of America*, 117(34), 20438–20446. <https://doi.org/10.1073/pnas.1916387117>
- Hugelius, G., Strauss, J., Zubrzycki, S., Harden, J. W., Schuur, E. A. G., Ping, C.-L., Schirmer, L., Grosse, G., Michaelson, G. J., Koven, C. D., O'Donnell, J. A., Elberling, B., Mishra, U., Camill, P., Yu, Z., Palmtag, J., & Kuhry, P. (2014). Estimated stocks of circumpolar permafrost carbon with quantified uncertainty ranges and identified data gaps. *Biogeosciences*, 11(23), 6573–6593. <https://doi.org/10.5194/bg-11-6573-2014>
- Jones, B. M., Grosse, G., Farquhar, L. M., Roy-Léveillé, P., Veremeeva, A., Kanevskiy, M. Z., Gaglioti, B. V., Breen, A. L., Parsekian, A. D., Ulrich, M., & Hinkel, K. M. (2022). Lake and drained lake basin systems in lowland permafrost regions. *Nature Reviews Earth and Environment*, 3(1), 85–98. <https://doi.org/10.1038/s43017-021-00238-9>
- Juncher Jørgensen, C., Lund Johansen, K. M., Westergaard-Nielsen, A., & Elberling, B. (2014). Net regional methane sink in High Arctic soils of northeast Greenland. *Nature Geoscience*, 8(1), 20–23. <https://doi.org/10.1038/ngeo2305>
- Kane, E. S., Chivers, M. R., Turetsky, M. R., Treat, C. C., Petersen, D. G., Waldrop, M., Harden, J. W., & McGuire, A. D. (2013). Response of anaerobic carbon cycling to water table manipulation in an Alaskan rich fen. *Soil Biology and Biochemistry*, 58, 50–60. <https://doi.org/10.1016/j.soilbio.2012.10.032>
- Kane, E. S., Dieleman, C. M., Rupp, D., Wyatt, K. H., Rober, A. R., & Turetsky, M. R. (2021). Consequences of increased variation in peatland hydrology for carbon storage: Legacy effects of drought and flood in a boreal fen ecosystem. *Frontiers in Earth Science*, 8, 577746. <https://www.frontiersin.org/article/10.3389/feart.2020.577746>
- Keuper, F., Wild, B., Kumm, M., Beer, C., Blume-Werry, G., Fontaine, S., Gavazov, K., Gentsch, N., Guggenberger, G., Hugelius, G., Jalava, M., Koven, C., Krab, E. J., Kuhry, P., Monteux, S., Richter, A., Shahzad, T., Weedon, J. T., & Dorrepaal, E. (2020). Carbon loss from northern circumpolar permafrost soils amplified by rhizosphere priming. *Nature Geoscience*, 13(8), 560–565. <https://doi.org/10.1038/s41561-020-0607-0>

- Khvorostyanov, D. V., Krinner, G., Ciais, P., Heimann, M., & Zimov, S. A. (2008). Vulnerability of permafrost carbon to global warming. Part I: Model description and role of heat generated by organic matter decomposition. *Tellus B: Chemical and Physical Meteorology*, 60(2), 250–264. <https://doi.org/10.1111/j.1600-0889.2007.00333.x>
- Kirtman, B., Power, S. B., Adedoyin, J. A., Boer, G. J., Bojariu, R., Camilloni, I., Doblas-Reyes, F. J., Fiore, A. M., Kimoto, M., Meehl, G. A., Prather, M., Sarr, A., Schär, C., Sutton, R., van Oldenborgh, G. J., Vecchi, G., & Wan, H. J. (2013). Near-term climate change: Projections and predictability. In T. F. Stocker, D. Qin, G.-K. Plattner, M. M. B. Tignor, S. K. Allen, J. Boschung, A. Nauels, Y. Xia, V. Bex, & P. M. Midgley (Eds.), *Climate Change 2013: The physical science basis. Contribution of Working Group I to the fifth assessment report of the Intergovernmental Panel on Climate Change* (pp. 953–1028). Cambridge University Press.
- Kittler, F., Burjack, I., Corradi, C. A. R., Heimann, M., Kolle, O., Merbold, L., Zimov, N., Zimov, S., & Göckede, M. (2016). Impacts of a decadal drainage disturbance on surface-atmosphere fluxes of carbon dioxide in a permafrost ecosystem. *Biogeosciences*, 13(18), 5315–5332. <https://doi.org/10.5194/bg-13-5315-2016>
- Kittler, F., Heimann, M., Kolle, O., Zimov, N., Zimov, S., & Göckede, M. (2017). Long-term drainage reduces CO<sub>2</sub> uptake and CH<sub>4</sub> emissions in a Siberian permafrost ecosystem. *Global Biogeochemical Cycles*, 31(12), 1704–1717. <https://doi.org/10.1002/2017GB005774>
- Kleinen, T., Brovkin, V., & Schuldt, R. J. (2012). A dynamic model of wetland extent and peat accumulation: Results for the Holocene. *Biogeosciences*, 9(1), 235–248. <https://doi.org/10.5194/bg-9-235-2012>
- Kobayashi, K., & Salam, M. U. (2000). Comparing simulated and measured values using mean squared deviation and its components. *Agronomy Journal*, 92(2), 345–352. <https://doi.org/10.2134/agronj2000.922345x>
- Kreyling, J., Tanneberger, F., Jansen, F., van der Linden, S., Aggenbach, C., Blüml, V., Couwenberg, J., Emsens, W.-J., Joosten, H., Klimkowska, A., Kotowski, W., Kozub, L., Lennartz, B., Liczner, Y., Liu, H., Michaelis, D., Oehmke, C., Parakenings, K., Pleyl, E., ... Jurasinski, G. (2021). Rewetting does not return drained fen peatlands to their old selves. *Nature Communications*, 12(1), 5693. <https://doi.org/10.1038/s41467-021-25619-y>
- Krinner, G., Viovy, N., de Noblet-Ducoudré, N., Ogée, J., Polcher, J., Friedlingstein, P., Ciais, P., Sitch, S., & Prentice, I. C. (2005). A dynamic global vegetation model for studies of the coupled atmosphere-biosphere system. *Global Biogeochemical Cycles*, 19(1), GB1015. <https://doi.org/10.1029/2003GB002199>
- Krüger, J. P., Alewell, C., Minkinen, K., Szidat, S., & Leifeld, J. (2016). Calculating carbon changes in peat soils drained for forestry with four different profile-based methods. *Forest Ecology and Management*, 381, 29–36. <https://doi.org/10.1016/j.foreco.2016.09.006>
- Kuhn, M. A., Varner, R. K., Bastviken, D., Crill, P., MacIntyre, S., Turetsky, M., Walter Anthony, K., McGuire, A. D., & Olefeldt, D. (2021). BAWLD-CH4: A comprehensive dataset of methane fluxes from boreal and arctic ecosystems. *Earth System Science Data*, 13(11), 5151–5189. <https://doi.org/10.5194/essd-13-5151-2021>
- Kwon, M. J., Beulig, F., Ille, I., Wildner, M., Küsel, K., Merbold, L., Mahecha, M., Zimov, N., Zimov, S. A., Heimann, M., Schuur, E. A. G., Kostka, J., Kolle, O., Hilke, I., & Göckede, M. (2017). Plants, microorganisms and soil temperatures contribute to a decrease in methane fluxes on a drained Arctic floodplain. *Global Change Biology*, 23(6), 2396–2412. <https://doi.org/10.1111/gcb.13558>
- Kwon, M. J., Heimann, M., Kolle, O., Luus, K. A., Schuur, E. A. G., Zimov, N., Zimov, S. A., & Göckede, M. (2016). Long-term drainage reduces CO<sub>2</sub> uptake and increases CO<sub>2</sub> emission on a Siberian floodplain due to shifts in vegetation community and soil thermal characteristics. *Biogeosciences*, 13, 4219–4235. <https://doi.org/10.5194/bg-13-4219-2016>
- Kwon, M. J., Natali, S. M., Hicks Pries, C. E., Schuur, E. A. G., Steinhof, A., Crummer, K. G., Zimov, N., Zimov, S. A., Heimann, M., Kolle, O., & Göckede, M. (2019). Drainage enhances modern soil carbon contribution but reduces old soil carbon contribution to ecosystem respiration in tundra ecosystems. *Global Change Biology*, 25(4), 1315–1325. <https://doi.org/10.1111/gcb.14578>
- Kwon, M. J., Tripathi, B. M., Göckede, M., Shin, S. C., Myeong, N. R., Lee, Y. K., & Kim, M. (2021). Disproportionate microbial responses to decadal drainage on a Siberian floodplain. *Global Change Biology*, 27(20), 5124–5140. <https://doi.org/10.1111/gcb.15785>
- Laiho, R., Vasander, H., Penttilä, T., & Laine, J. (2003). Dynamics of plant-mediated organic matter and nutrient cycling following water-level drawdown in boreal peatlands. *Global Biogeochemical Cycles*, 17(2), 1053. <https://doi.org/10.1029/2002GB002015>
- Laine, J., Silvola, J., Tolonen, K., Alm, J., Nykänen, H., Vasander, H., Sallantausta, T., Savolainen, I., Sinisalo, J., & Martikainen, P. (1996). Effect of water-level drawdown on global climatic warming: Northern peatlands. *Ambio*, 25(3), 179–184.
- Lara, M. J., McGuire, A. D., Euskirchen, E. S., Tweedie, C. E., Hinkel, K. M., Skurikhin, A. N., Romanovsky, V. E., Grosse, G., Bolton, W. R., & Genet, H. (2015). Polygonal tundra geomorphological change in response to warming alters future CO<sub>2</sub> and CH<sub>4</sub> flux on the Barrow Peninsula. *Global Change Biology*, 21(4), 1634–1651. <https://doi.org/10.1111/gcb.12757>
- Lawrence, D. M., Koven, C. D., Swenson, S. C., Riley, W. J., & Slater, A. G. (2015). Permafrost thaw and resulting soil moisture changes regulate projected high-latitude CO<sub>2</sub> and CH<sub>4</sub> emissions. *Environmental Research Letters*, 10(9), 094011. <https://doi.org/10.1088/1748-9326/10/9/094011>
- Leifeld, J., & Menichetti, L. (2018). The underappreciated potential of peatlands in global climate change mitigation strategies. *Nature Communications*, 9(1), 1071. <https://doi.org/10.1038/s41467-018-03406-6>
- Leifeld, J., Wüst-Galley, C., & Page, S. (2019). Intact and managed peatland soils as a source and sink of GHGs from 1850 to 2100. *Nature Climate Change*, 9(12), 945–947. <https://doi.org/10.1038/s41558-019-0615-5>
- Lewis, K. C., Zyzolowski, G. A., Travis, B., Wilson, C., & Rowland, J. (2012). Drainage subsidence associated with Arctic permafrost degradation. *Journal of Geophysical Research: Earth Surface*, 117(F4), F04019. <https://doi.org/10.1029/2011JF002284>
- Liljedahl, A. K., Boike, J., Daanen, R. P., Fedorov, A. N., Frost, G. V., Grosse, G., Hinzman, L. D., Iijima, Y., Jorgenson, J. C., Matveyeva, N., Necsoiu, M., Reynolds, M. K., Romanovsky, V. E., Schulla, J., Tape, K. D., Walker, D. A., Wilson, C. J., Yabuki, H., & Zona, D. (2016). Pan-Arctic ice-wedge degradation in warming permafrost and its influence on tundra hydrology. *Nature Geoscience*, 9, 312–318. <https://doi.org/10.1038/ngeo2674>
- Lynch, J., Cain, M., Pierrehumbert, R., & Allen, M. (2020). Demonstrating GWP\*: A means of reporting warming-equivalent emissions that captures the contrasting impacts of short- and long-lived climate pollutants. *Environmental Research Letters*, 15(4), 044023. <https://doi.org/10.1088/1748-9326/ab6d7e>
- MacDonald, G. M., Beilman, D. W., Kremenetski, K. V., Sheng, Y., Smith, L. C., & Velichko, A. A. (2006). Rapid early development of circumarctic peatlands and atmospheric CH<sub>4</sub> and CO<sub>2</sub> variations. *Science*, 314(5797), 285–288. <https://doi.org/10.1126/science.1131722>
- Martikainen, P. J., Nykänen, H., Alm, J., & Silvola, J. (1995). Change in fluxes of carbon dioxide, methane and nitrous oxide due to forest drainage of mire sites of different trophic. *Plant and Soil*, 168(1), 571–577. <https://doi.org/10.1007/BF00029370>
- McCarter, C. P. R., Rezanezhad, F., Quinton, W. L., Gharedaghloo, B., Lennartz, B., Price, J., Connon, R., & Van Cappellen, P. (2020). Pore-scale controls on hydrological and geochemical processes in peat: Implications on interacting processes. *Earth-Science Reviews*, 207, 103227. <https://doi.org/10.1016/j.earscirev.2020.103227>

- McPartland, M. Y., Kane, E. S., Falkowski, M. J., Kolka, R., Turetsky, M. R., Palik, B., & Montgomery, R. A. (2019). The response of boreal peatland community composition and NDVI to hydrologic change, warming, and elevated carbon dioxide. *Global Change Biology*, 25(1), 93–107. <https://doi.org/10.1111/gcb.14465>
- Minkinen, K., Vasander, H., Jauhiainen, S., Karsisto, M., & Laine, J. (1999). Post-drainage changes in vegetation composition and carbon balance in Lakkasuo mire, Central Finland. *Plant and Soil*, 207(1), 107–120.
- Morel, X., Decharme, B., Delire, C., Krinner, G., Lund, M., Hansen, B. U., & Mastepanov, M. (2019). A new process-based soil methane scheme: Evaluation over arctic field sites with the ISBA land surface model. *Journal of Advances in Modeling Earth Systems*, 11(1), 293–326. <https://doi.org/10.1029/2018MS001329>
- Moyano, F. E., Manzoni, S., & Chenu, C. (2013). Responses of soil heterotrophic respiration to moisture availability: An exploration of processes and models. *Soil Biology and Biochemistry*, 59, 72–85. <https://doi.org/10.1016/j.soilbio.2013.01.002>
- Muhr, J., Höhle, J., Otieno, D. O., & Borken, W. (2011). Manipulative lowering of the water table during summer does not affect CO<sub>2</sub> emissions and uptake in a fen in Germany. *Ecological Applications: A Publication of the Ecological Society of America*, 21(2), 391–401. <https://doi.org/10.1890/09-1251.1>
- Murphy, M., Laiho, R., & Moore, T. R. (2009). Effects of water table drawdown on root production and aboveground biomass in a boreal bog. *Ecosystems*, 12(8), 1268–1282. <https://doi.org/10.1007/s10021-009-9283-z>
- Natali, S. M., Schuur, E. A. G., Mauritz, M., Schade, J., Celis, G., Crummer, G., Johnston, C., Krapek, J., Pegoraro, E., Salmon, V., & Webb, E. (2015). Permafrost thaw and soil moisture drive CO<sub>2</sub> and CH<sub>4</sub> release from upland tundra. *Journal of Geophysical Research: Biogeosciences*, 120(3), 525–537. <https://doi.org/10.1002/2014JG002872>
- Natali, S. M., Watts, J. D., Rogers, B. M., Potter, S., Ludwig, S. M., Selbmann, A.-K., Sullivan, P. F., Abbott, B. W., Arndt, K. A., Birch, L., Björkman, M. P., Bloom, A. A., Celis, G., Christensen, T. R., Christiansen, C. T., Commann, R., Cooper, E. J., Crill, P., Czimczik, C., ... Zona, D. (2019). Large loss of CO<sub>2</sub> in winter observed across the northern permafrost region. *Nature Climate Change*, 9(11), 852–857. <https://doi.org/10.1038/s41558-019-0592-8>
- Nichols, J. E., & Peteet, D. M. (2019). Rapid expansion of northern peatlands and doubled estimate of carbon storage. *Nature Geoscience*, 12(11), 917–921. <https://doi.org/10.1038/s41561-019-0454-z>
- Nichols, J. E., & Peteet, D. M. (2021). J. E. Nichols and D. M. Peteet reply. *Nature Geoscience*, 14(7), 470–472. <https://doi.org/10.1038/s41561-021-00771-8>
- Nijp, J. J., Metselaar, K., Limpens, J., Teutschbein, C., Peichl, M., Nilsson, M. B., Berendse, F., & van der Zee, S. E. A. T. M. (2017). Including hydrological self-regulating processes in peatland models: Effects on peatmoss drought projections. *Science of the Total Environment*, 580, 1389–1400. <https://doi.org/10.1016/j.scitotenv.2016.12.104>
- Nitzbon, J., Westermann, S., Langer, M., Martin, L. C. P., Strauss, J., Laboor, S., & Boike, J. (2020). Fast response of cold ice-rich permafrost in northeast Siberia to a warming climate. *Nature Communications*, 11(1), 2201. <https://doi.org/10.1038/s41467-020-15725-8>
- Nykänen, H., Alm, J., Silvola, J., Tolonen, K., & Martikainen, P. J. (1998). Methane fluxes on boreal peatlands of different fertility and the effect of long-term experimental lowering of the water table on flux rates. *Global Biogeochemical Cycles*, 12(1), 53–69. <https://doi.org/10.1029/97gb02732>
- Nykänen, H., Rissanen, A. J., Turunen, J., Tahvanainen, T., & Simola, H. (2020). Carbon storage change and  $\delta^{13}\text{C}$  transitions of peat columns in a partially forestry-drained boreal bog. *Plant and Soil*, 447(1), 365–378. <https://doi.org/10.1007/s11104-019-04375-5>
- Oh, Y., Zhuang, Q., Liu, L., Welp, L. R., Lau, M. C. Y., Onstott, T. C., Medvigy, D., Bruhwiler, L., Dlugokencky, E. J., Hugelius, G., D'Imperio, L., & Elberling, B. (2020). Reduced net methane emissions due to microbial methane oxidation in a warmer Arctic. *Nature Climate Change*, 10(4), 317–321. <https://doi.org/10.1038/s41558-020-0734-z>
- Olefeldt, D., Euskirchen, E. S., Harden, J., Kane, E. S., McGuire, A. D., Waldrop, M. P., & Turetsky, M. R. (2017). A decade of boreal rich fen greenhouse gas fluxes in response to natural and experimental water table variability. *Global Change Biology*, 23(6), 2428–2440. <https://doi.org/10.1111/gcb.13612>
- Olefeldt, D., Goswami, S., Grosse, G., Hayes, D., Hugelius, G., Kuhry, P., McGuire, A. D., Romanovsky, V. E., Sannel, A. B. K., Schuur, E. A. G., & Turetsky, M. R. (2016). Circumpolar distribution and carbon storage of thermokarst landscapes. *Nature Communications*, 7(1), 13043. <https://doi.org/10.1038/ncomms13043>
- Olefeldt, D., Hovemyr, M., Kuhn, M. A., Bastviken, D., Bohn, T. J., Connolly, J., Crill, P., Euskirchen, E. S., Finkelstein, S. A., Genet, H., Grosse, G., Harris, L. I., Heffernan, L., Helbig, M., Hugelius, G., Hutchins, R., Juutinen, S., Lara, M. J., Malhotra, A., ... Watts, J. D. (2021). The Boreal–Arctic wetland and lake dataset (BAWLD). *Earth System Science Data*, 13(11), 5127–5149. <https://doi.org/10.5194/essd-13-5127-2021>
- Olefeldt, D., Turetsky, M. R., Crill, P. M., & McGuire, A. D. (2013). Environmental and physical controls on northern terrestrial methane emissions across permafrost zones. *Global Change Biology*, 19(2), 589–603. <https://doi.org/10.1111/gcb.12071>
- O'Neill, H. B., Wolfe, S. A., & Duchesne, C. (2019). New ground ice maps for Canada using a paleogeographic modelling approach. *The Cryosphere*, 13(3), 753–773. <https://doi.org/10.5194/tc-13-753-2019>
- Palmer, T. N., & Räisänen, J. (2002). Quantifying the risk of extreme seasonal precipitation events in a changing climate. *Nature*, 415(6871), 512–514. <https://doi.org/10.1038/415512a>
- Parton, W. J., Schimel, D. S., Cole, C. V., & Ojima, D. S. (1987). Analysis of factors controlling soil organic matter levels in Great Plains grasslands. *Soil Science Society of America Journal*, 51(5), 1173–1179. <https://doi.org/10.2136/sssaj1987.03615995005100050015x>
- Paustian, K., Parton, W. J., & Persson, J. (1992). Modeling soil organic matter in organic-amended and nitrogen-fertilized long-term plots. *Soil Science Society of America Journal*, 56(2), 476–488. <https://doi.org/10.2136/sssaj1992.03615995005600020023x>
- Potvin, L. R., Kane, E. S., Chimner, R. A., Kolka, R. K., & Lilleskov, E. A. (2015). Effects of water table position and plant functional group on plant community, aboveground production, and peat properties in a peatland mesocosm experiment (PEATcosm). *Plant and Soil*, 387(1–2), 277–294. <https://doi.org/10.1007/s11104-014-2301-8>
- Qiu, C., Ciais, P., Zhu, D., Guenet, B., Chang, J., Chaudhary, N., Kleinen, T., Li, X., Müller, J., Xi, Y., Zhang, W., Ballantyne, A., Brewer, S. C., Brovkin, V., Charman, D. J., Gustafson, A., Gallego-Sala, A. V., Gasser, T., Holden, J., ... Westermann, S. (2022). A strong mitigation scenario maintains climate neutrality of northern peatlands. *One Earth*, 5(1), 86–97. <https://doi.org/10.1016/j.oneear.2021.12.008>
- Qiu, C., Zhu, D., Ciais, P., Guenet, B., Krinner, G., Peng, S., Aurela, M., Bernhofer, C., Brümmer, C., Bret-Harte, S., Chu, H., Chen, J., Desai, A. R., Dušek, J., Euskirchen, E. S., Fortuniak, K., Flanagan, L. B., Friborg, T., Grygoruk, M., ... Ziemblinska, K. (2018). ORCHIDEE-PEAT (revision 4596), a model for northern peatland CO<sub>2</sub>, water, and energy fluxes on daily to annual scales. *Geoscientific Model Development*, 11(2), 497–519. <https://doi.org/10.5194/gmd-11-497-2018>
- Qiu, C., Zhu, D., Ciais, P., Guenet, B., Peng, S., Krinner, G., Tootchi, A., Ducharne, A., & Hastie, A. (2019). Modelling northern peatland area and carbon dynamics since the Holocene with the ORCHIDEE-PEAT land surface model (SVN r5488). *Geoscientific Model Development*, 12(7), 2961–2982. <https://doi.org/10.5194/gmd-12-2961-2019>



- R Development Core Team. (2013). *R: A language and environment for statistical computing*. R Foundation for Statistical Computing. <http://www.r-project.org>
- Ratcliffe, J. L., Peng, H., Nijp, J. J., & Nilsson, M. B. (2021). Lateral expansion of northern peatlands calls into question a 1,055 GtC estimate of carbon storage. *Nature Geoscience*, 14(7), 468–469. <https://doi.org/10.1038/s41561-021-00770-9>
- Riley, W. J., Subin, Z. M., Lawrence, D. M., Swenson, S. C., Torn, M. S., Meng, L., Mahowald, N. M., & Hess, P. (2011). Barriers to predicting changes in global terrestrial methane fluxes: Analyses using CLM4Me, a methane biogeochemistry model integrated in CESM. *Biogeosciences*, 8(7), 1925–1953. <https://doi.org/10.5194/bg-8-1925-2011>
- Rodenhizer, H., Ledman, J., Mauritz, M., Natali, S. M., Pegoraro, E., Plaza, C., Romano, E., Schädel, C., Taylor, M., & Schuur, E. (2020). Carbon thaw rate doubles when accounting for subsidence in a permafrost warming experiment. *Journal of Geophysical Research: Biogeosciences*, 125(6), e2019JG005528. <https://doi.org/10.1029/2019JG005528>
- Roy Chowdhury, T., Berns, E. C., Moon, J.-W., Gu, B., Liang, L., Wullschlegel, S. D., & Graham, D. E. (2021). Temporal, spatial, and temperature controls on organic carbon mineralization and methanogenesis in Arctic High-centered polygon soils. *Frontiers in Microbiology*, 11, 3414. <https://doi.org/10.3389/fmicb.2020.616518>
- Rupp, D. L., Lamit, L. J., Techtmann, S. M., Kane, E. S., Lilleskov, E. A., & Turetsky, M. R. (2021). The rhizosphere responds: Rich fen peat and root microbial ecology after long-term water table manipulation. *Applied and Environmental Microbiology*, 87(12), e00241–e00221. <https://doi.org/10.1128/AEM.00241-21>
- Saarnio, S., Alm, J., Silvola, J., Lohila, A., Nykänen, H., & Martikainen, P. J. (1997). Seasonal variation in CH<sub>4</sub> emissions and production and oxidation potentials at microsites on an oligotrophic pine fen. *Oecologia*, 110(3), 414–422. <https://doi.org/10.1007/s004420050176>
- Salmon, E., Jégou, F., Guenet, B., Jourdain, L., Qiu, C., Bastrov, V., Guimbaud, C., Zhu, D., Ciais, P., Peylin, P., Gogo, S., Laggoun-Défarge, F., Aurela, M., Bret-Harte, M. S., Chen, J., Chojnicki, B. H., Chu, H., Edgar, C. W., Euskirchen, E. S., ... Ziemlińska, K. (2021). Assessing methane emissions for northern peatlands in ORCHIDEE-PEAT revision 7020. *Geoscientific Model Development Discussions*, 15(7), 2813–2838. <https://doi.org/10.5194/gmd-2021-280>
- Schuur, E. A. G., McGuire, A. D., Schädel, C., Grosse, G., Harden, J. W., Hayes, D. J., Hugelius, G., Koven, C. D., Kuhry, P., Lawrence, D. M., Natali, S. M., Olefeldt, D., Romanovsky, V. E., Schaefer, K., Turetsky, M. R., Treat, C. C., & Vonk, J. E. (2015). Climate change and the permafrost carbon feedback. *Nature*, 520, 171–179. <https://doi.org/10.1038/nature14338>
- Shiogama, H., Imada, Y., Mori, M., Mizuta, R., Stone, D., Yoshida, K., Arakawa, O., Ikeda, M., Takahashi, C., Arai, M., Ishii, M., Watanabe, M., & Kimoto, M. (2016). Attributing historical changes in probabilities of record-breaking daily temperature and precipitation extreme events. *SOLA*, 12, 225–231. <https://doi.org/10.2151/sola.2016-045>
- Simola, H., Pitkänen, A., & Turunen, J. (2012). Carbon loss in drained forestry peatlands in Finland, estimated by re-sampling peatlands surveyed in the 1980s. *European Journal of Soil Science*, 63(6), 798–807. <https://doi.org/10.1111/j.1365-2389.2012.01499.x>
- Soudzilovskaia, N. A., van Bodegom, P. M., & Cornelissen, J. H. C. (2013). Dominant bryophyte control over high-latitude soil temperature fluctuations predicted by heat transfer traits, field moisture regime and laws of thermal insulation. *Functional Ecology*, 27(6), 1442–1454.
- Sulman, B. N., Desai, A. R., Saliendra, N. Z., Lafleur, P. M., Flanagan, L. B., Sonnentag, O., Mackay, D. S., Barr, A. G., & van der Kamp, G. (2010). CO<sub>2</sub> fluxes at northern fens and bogs have opposite responses to inter-annual fluctuations in water table. *Geophysical Research Letters*, 37(19), L19702. <https://doi.org/10.1029/2010GL044018>
- Swindles, G. T., Morris, P. J., Mullan, D. J., Payne, R. J., Roland, T. P., Amesbury, M. J., Lamentowicz, M., Turner, T. E., Gallego-Sala, A., Sim, T., Barr, I. D., Blaauw, M., Blundell, A., Chambers, F. M., Charman, D. J., Feurdean, A., Galloway, J. M., Gałka, M., Green, S. M., ... Warner, B. (2019). Widespread drying of European peatlands in recent centuries. *Nature Geoscience*, 12(11), 922–928. <https://doi.org/10.1038/s41561-019-0462-z>
- Tarnocai, C., Canadell, J. G., Schuur, E. A. G., Kuhry, P., Mazhitova, G., & Zimov, S. (2009). Soil organic carbon pools in the northern circumpolar permafrost region. *Global Biogeochemical Cycles*, 23(2), GB2023.
- Treat, C. C., Bloom, A. A., & Marushchak, M. E. (2018). Nongrowing season methane emissions—a significant component of annual emissions across northern ecosystems. *Global Change Biology*, 24(8), 3331–3343. <https://doi.org/10.1111/gcb.14137>
- Treat, C. C., Jones, M. C., Alder, J., Sannel, A. B. K., Camill, P., & Frohling, S. (2021). Predicted vulnerability of carbon in permafrost peatlands with future climate change and permafrost thaw in western Canada. *Journal of Geophysical Research: Biogeosciences*, 126(5), e2020JG005872. <https://doi.org/10.1029/2020JG005872>
- Treat, C. C., Kleinen, T., Brothoerts, N., Dalton, A. S., Dommain, R., Douglas, T. A., Drexler, J. Z., Finkelstein, S. A., Grosse, G., Hope, G., Hutchings, J., Jones, M. C., Kuhry, P., Lacourse, T., Lähteenoja, O., Loisel, J., Notebaert, B., Payne, R. J., Peteet, D. M., ... Brovkin, V. (2019). Widespread global peatland establishment and persistence over the last 130,000 y. *Proceedings of the National Academy of Sciences of the United States of America*, 116(11), 4822–4827. <https://doi.org/10.1073/pnas.1813305116>
- Turetsky, M. R., Donahue, W. F., & Benschoter, B. W. (2011). Experimental drying intensifies burning and carbon losses in a northern peatland. *Nature Communications*, 2(1), 514. <https://doi.org/10.1038/ncomm1523>
- Turetsky, M. R., Kotowska, A., Bubier, J., Dise, N. B., Crill, P., Hornibrook, E. R. C., Minkinen, K., Moore, T. R., Myers-Smith, I. H., Nykänen, H., Olefeldt, D., Rinne, J., Saarnio, S., Shurpali, N., Tuittila, E.-S., Waddington, J. M., White, J. R., Wickland, K. P., & Wilking, M. (2014). A synthesis of methane emissions from 71 northern, temperate, and subtropical wetlands. *Global Change Biology*, 20(7), 2183–2197. <https://doi.org/10.1111/gcb.12580>
- Turetsky, M. R., Treat, C. C., Waldrop, M. P., Waddington, J. M., Harden, J. W., & McGuire, A. D. (2008). Short-term response of methane fluxes and methanogen activity to water table and soil warming manipulations in an Alaskan peatland. *Journal of Geophysical Research*, 113, G00A10. <https://doi.org/10.1029/2007JG000496>
- Ukkola, A. M., Kauwe, M. G. D., Roderick, M. L., Abramowitz, G., & Pitman, A. J. (2020). Robust future changes in meteorological drought in CMIP6 projections despite uncertainty in precipitation. *Geophysical Research Letters*, 47(11), e2020GL087820. <https://doi.org/10.1029/2020GL087820>
- Vaughn, L. J. S., Conrad, M. E., Bill, M., & Torn, M. S. (2016). Isotopic insights into methane production, oxidation, and emissions in Arctic polygon tundra. *Global Change Biology*, 22(10), 3487–3502. <https://doi.org/10.1111/gcb.13281>
- Virkkala, A.-M., Aalto, J., Rogers, B. M., Tagesson, T., Treat, C. C., Natali, S. M., Watts, J. D., Potter, S., Lehtonen, A., Mauritz, M., Schuur, E. A. G., Kochendorfer, J., Zona, D., Oechel, W., Kobayashi, H., Humphreys, E., Goekede, M., Iwata, H., Lafleur, P. M., ... Luoto, M. (2021). Statistical upscaling of ecosystem CO<sub>2</sub> fluxes across the terrestrial tundra and boreal domain: Regional patterns and uncertainties. *Global Change Biology*, 27(17), 4040–4059. <https://doi.org/10.1111/gcb.15659>
- Waddington, J. M., Harrison, K., Kellner, E., & Baird, A. J. (2009). Effect of atmospheric pressure and temperature on entrapped gas content in peat. *Hydrological Processes*, 23(20), 2970–2980. <https://doi.org/10.1002/hyp.7412>

- Waddington, J. M., Morris, P. J., Kettridge, N., Granath, G., Thompson, D. K., & Moore, P. A. (2015). Hydrological feedbacks in northern peatlands. *Ecohydrology*, 8(1), 113–127. <https://doi.org/10.1002/eco.1493>
- Wainwright, H. M., Dafflon, B., Smith, L. J., Hahn, M. S., Curtis, J. B., Wu, Y., Ulrich, C., Peterson, J. E., Torn, M. S., & Hubbard, S. S. (2015). Identifying multiscale zonation and assessing the relative importance of polygon geomorphology on carbon fluxes in an Arctic tundra ecosystem. *Journal of Geophysical Research: Biogeosciences*, 120(4), 788–808. [https://doi.org/10.1002/2014JG002799@10.1002/\(ISSN\)2169-9291.ARCTICJOINT](https://doi.org/10.1002/2014JG002799@10.1002/(ISSN)2169-9291.ARCTICJOINT)
- Walter, B. P., & Heimann, M. (2000). A process-based, climate-sensitive model to derive methane emissions from natural wetlands: Application to five wetland sites, sensitivity to model parameters, and climate. *Global Biogeochemical Cycles*, 14(3), 745–765. <https://doi.org/10.1029/1999GB001204>
- Wania, R., Ross, I., & Prentice, I. C. (2010). Implementation and evaluation of a new methane model within a dynamic global vegetation model: LPJ-WHyMe v1.3.1. *Geoscientific Model Development*, 3(2), 565–584. <https://doi.org/10.5194/gmd-3-565-2010>
- Ward, N. D., Bianchi, T. S., Martin, J. B., Quintero, C. J., Sawakuchi, H. O., & Cohen, M. J. (2020). Pathways for methane emissions and oxidation that influence the net carbon balance of a subtropical cypress swamp. *Frontiers in Earth Science*, 8, 573357. <https://www.frontiersin.org/article/10.3389/feart.2020.573357>
- Wijedasa, L. S., Sloan, S., Page, S. E., Clements, G. R., Lupascu, M., & Evans, T. A. (2018). Carbon emissions from South-East Asian peatlands will increase despite emission-reduction schemes. *Global Change Biology*, 24(10), 4598–4613. <https://doi.org/10.1111/gcb.14340>
- Witze, A. (2020). The Arctic is burning like never before—And that's bad news for climate change. *Nature*, 585(7825), 336–337. <https://doi.org/10.1038/d41586-020-02568-y>
- Wu, J., Roulet, N. T., Sagerfors, J., & Nilsson, M. B. (2013). Simulation of six years of carbon fluxes for a sedge-dominated oligotrophic minerogenic peatland in Northern Sweden using the McGill Wetland Model (MWM). *Journal of Geophysical Research: Biogeosciences*, 118(2), 795–807. <https://doi.org/10.1002/jgrg.20045>
- Wyatt, K. H., McCann, K. S., Rober, A. R., & Turetsky, M. R. (2021). Trophic interactions regulate peatland carbon cycling. *Ecology Letters*, 24(4), 781–790. <https://doi.org/10.1111/ele.13697>
- Xu, J., Morris, P. J., Liu, J., & Holden, J. (2018). PEATMAP: Refining estimates of global peatland distribution based on a meta-analysis. *Catena*, 160, 134–140. <https://doi.org/10.1016/j.catena.2017.09.010>
- Yu, Z., Joos, F., Bauska, T. K., Stocker, B. D., Fischer, H., Loisel, J., Brovkin, V., Hugelius, G., Nehrbass-Ahles, C., Kleinen, T., & Schmitt, J. (2021). No support for carbon storage of >1,000 GtC in northern peatlands. *Nature Geoscience*, 14(7), 465–467. <https://doi.org/10.1038/s41561-021-00769-2>
- Yu, Z., Loisel, J., Brosseau, D. P., Beilman, D. W., & Hunt, S. J. (2010). Global peatland dynamics since the Last Glacial Maximum. *Geophysical Research Letters*, 37(13), L13402. <https://doi.org/10.1029/2010GL043584>
- Zona, D., Lipson, D. A., Paw, K. T., Oberbauer, S. F., Olivas, P., Gioli, B., & Oechel, W. C. (2012). Increased CO<sub>2</sub> loss from vegetated drained lake tundra ecosystems due to flooding. *Global Biogeochemical Cycles*, 26, GB2004. <https://doi.org/10.1029/2011GB004037>
- Zona, D., Oechel, W. C., Kochendorfer, J., Paw, U. K. T., Salyuk, A. N., Olivas, P. C., Oberbauer, S. F., & Lipson, D. A. (2009). Methane fluxes during the initiation of a large-scale water table manipulation experiment in the Alaskan Arctic tundra. *Global Biogeochemical Cycles*, 23, GB2013. <https://doi.org/10.1029/2009GB003487>

## SUPPORTING INFORMATION

Additional supporting information can be found online in the Supporting Information section at the end of this article.

**How to cite this article:** Kwon, M. J., Ballantyne, A., Ciais, P., Qiu, C., Salmon, E., Raoult, N., Guenet, B., Göckede, M., Euskirchen, E. S., Nykänen, H., Schuur, E. A. G., Turetsky, M. R., Dieleman, C. M., Kane, E. S., & Zona, D. (2022). Lowering water table reduces carbon sink strength and carbon stocks in northern peatlands. *Global Change Biology*, 28, 6752–6770. <https://doi.org/10.1111/gcb.16394>